# An Estimate of Increases in Storm Surge Risk to Property from Sea Level Rise in the First Half of the Twenty-First Century

ROSS N. HOFFMAN,* PETER DAILEY,+ SUSANNA HOPSCH,*,+ RUI M. PONTE,* KATHERINE QUINN,* EMMA M. HILL,#,@ AND BRIAN ZACHRY+

* *Atmospheric and Environmental Research, Inc., Lexington, Massachusetts*
+ *AIR Worldwide Corp., Boston, Massachusetts*
# *Harvard-Smithsonian Center for Astrophysics, Cambridge, Massachusetts*

(Manuscript received 8 December 2009, in final form 26 October 2010)

ABSTRACT

Sea level is rising as the World Ocean warms and ice caps and glaciers melt. Published estimates based on data from satellite altimeters, beginning in late 1992, suggest that the global mean sea level has been rising on the order of 3 mm $yr^{-1}$. Local processes, including ocean currents and land motions due to a variety of causes, modulate the global signal spatially and temporally. These local signals can be much larger than the global signal, and especially so on annual or shorter time scales.

Even increases on the order of 10 cm in sea level can amplify the already devastating losses that occur when a hurricane-driven storm surge coincides with an astronomical high tide. To quantify the sensitivity of property risk to increasing sea level, changes in expected annual losses to property along the U.S. Gulf and East Coasts are calculated as follows. First, observed trends in sea level rise from tide gauges are extrapolated to the year 2030, and these changes are interpolated to all coastal locations. Then a 10 000-yr catalog of simulated hurricanes is used to define critical wind parameters for each event. These wind parameters then drive a parametric time-evolving storm surge model that accounts for bathymetry, coastal geometry, surface roughness, and the phase of the astronomical tide. The impact of the maximum storm surge height on a comprehensive inventory of commercial and residential property is then calculated, using engineering models that take into account the characteristics of the full range of construction types.

Average annual losses projected to the year 2030 are presented for regions and key states and are normalized by aggregate property value on a zip code by zip code basis. Comparisons to the results of a control run reflecting the risk today quantify the change in risk per dollar of property on a percentage basis. Increases in expected losses due to the effect of sea level rise alone vary by region, with increases of 20% or more being common. Further sensitivity tests quantify the impact on the risk of sea level rise plus additional factors, such as changes in hurricane frequency and intensity as a result of rising sea surface temperatures.

## 1. Introduction

Sea level is projected to continue to rise, and some studies suggest that the rate of rise is accelerating (e.g., Church and White 2006). Since even a difference on the order of 10 cm in the astronomical tide can have a significant impact on storm surge risk to life and property, sea level rise is directly connected to storm surge risk. Furthermore, although consideration of local sea level involves several complicating factors as described in section 2, the connection between sea level rise and climate change has fewer associated ambiguities and uncertainties than other factors, such as patterns of precipitation. Therefore, the impact of sea level change on storm surge risk is both of great importance and amenable to study.

Projecting losses to property in the future as sea level rises is, however, not without difficulty. The first uncertainty is to project the future inventory of real estate along the coast. In addition to the value of these properties, impacts of trends in construction practices on property vulnerability to storm surge must be projected. Such projections in turn would require economic, social (i.e., population trend), and regulatory projections. These competing factors result in high levels of forecast uncertainty.

@ Current affiliation: Earth Observatory of Singapore, Nanyang Technological University, Singapore.

*Corresponding author address:* Dr. Ross N. Hoffman, Atmospheric and Environmental Research, Inc., 131 Hartwell Ave., Lexington, MA 02421–3126.
E-mail: rhoffman@aer.com

DOI: 10.1175/2010WCAS1050.1

Here we focus directly on property loss. To project insurance loss one would also have to project exposure, which in turn would depend on projecting underwriting trends as well as underlying property values. Another major uncertainty is how storm characteristics will change in the future.

As a preliminary sensitivity study, we quantify the change in expected risk under a scenario in which sea level is assumed to rise immediately by an amount equivalent to a conservative projection of sea level rise over 20 years. To accomplish this we first estimate how sea level has been rising as observed by tide gauges and extrapolate this trend to produce a map of sea level rise (section 2). Then we apply an advanced catastrophe model (CAT model) to evaluate the risk of hurricane storm surge to all existing residential and commercial real estate along the U.S. Gulf and East Coasts (section 3). (Appendix A is a glossary of insurance industry terms; appendix B provides a brief technical description of the AIR Worldwide Corp. U.S. Hurricane Catastrophe Model that is used in this study.) In practical applications of CAT modeling, probability estimates of risk due to a single or multiple hazards are made for the particular exposure of an individual insurer, accounting for the distribution of properties, their construction characteristics, and the policy language. In the present study, only hurricane storm surge damage is calculated and the risk is computed for all property rather than for the property covered by an individual insurer. The calculation is done for scenarios for current conditions, for current conditions with sea level increased, and for warm sea surface temperature (SST) conditions with sea level increased (section 4). This last case allows us to examine, albeit in isolation, the likely impact of one aspect of climate change on hurricane development. However, analysis of tide gauge observations along the U.S. East Coast (Zhang et al. 2000) and globally (Woodworth and Blackman 2004) does not indicate an increase in the statistics of extreme storm surge levels in the recent past.

CAT models are particularly well suited for the type of sensitivity study presented here because they use very large stochastic catalogs of tens of thousands of years of simulated hurricanes to provide precise probabilities of risk to property. This characteristic of CAT models allows us to elucidate fine details of risk and changes in risk under various scenarios of climate change. Since we do not forecast future values, we focus on risk ratios and changes in these ratios that result from different scenarios. There are several limitations of the current study (section 3), but there are also a number of interesting potential extensions (section 5).

There have been numerous studies examining the processes responsible for sea level rise and the effect of sea level rise on the environment and society (Solomon et al. 2007, and references therein). The Intergovernmental Panel on Climate Change Fourth Assessment Report (IPCC AR4) projections focus on average mean sea level rise expected at the end of the twenty-first century (2080–2100 relative to 1980–2000). Projected rise ranges between approximately 0.2 and 0.6 m, depending on the different models and scenarios used. A full account of uncertainties in ice sheet dynamics would lead to larger spreads. Similar IPCC projections on a regional basis yield differences mostly around $\pm 0.2$ m in local sea level rates arising solely from density and circulation changes. Spatial patterns are, nevertheless, very uncertain, as judged by the disagreement among various models (Solomon et al. 2007, Fig. 10.32), and are expected to be even more uncertain on the shorter (decadal) time scales of interest to us. In terms of economic effects, only limited research has addressed the potential financial impact of sea level rise on society from storm surge risk (e.g., McInnes et al. 2003; Hallegatte et al. 2008) because of the complexities in performing this type of analysis and in the underlying assumptions and uncertainties described above. Here we restrict ourselves to extrapolations of observed local trends in sea level to the year 2030. From these we estimate the sensitivity of storm surge risk to sea level rise and the associated financial impacts by calculating average annual storm surge losses for the entire U.S. East and Gulf Coasts.

## 2. Modeling sea level rise

In this section we describe how relative sea level variations, as measured at tide gauges, are analyzed to project sea level rise in the future. The analysis here is aimed toward estimating the observed rate of sea level rise at tide gauges along the U.S. Gulf and East Coasts. For the purpose of the surge model, described in section 3, these rates are then extrapolated and spatially interpolated to provide a projected increase in sea level in the year 2030.

Globally averaged sea level has been rising. Since 1993 we have excellent records from satellite altimeter missions. Before that time researchers have combined data from numerous tide gauges to determine the global (or eustatic) sea level variations. For example, three different estimates of global sea level changes are shown in Fig. 1, reproduced from Solomon et al. (2007, chapter 5).

A wide range of processes contribute to relative sea level changes. These processes cause significant spatial variations in sea level change and affect sea level on a variety of time scales. We categorize these processes as follows:

1) **Changes in mass.** The mass of the ocean may increase because of melting glaciers and ice sheets, increased

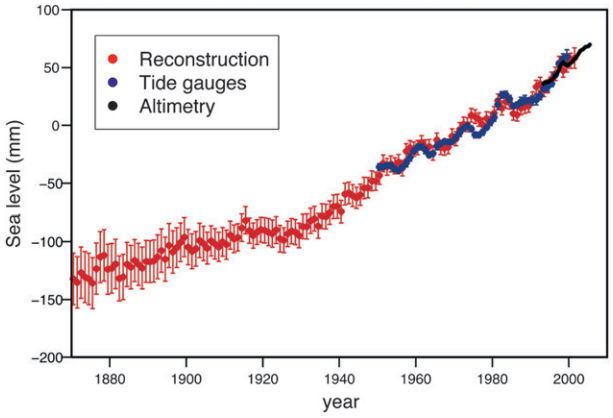


FIG. 1. Estimates of trends in global mean sea level (mm). Data plotted are annual averages from the reconstruction of Church and White (2006, red), coastal tide gauges from Holgate and Woodworth (2004, blue), and altimeter data from Leuliette et al. (2004, black). Values plotted are deviations from the mean for the 30-yr period ending in 1990 for the longer two datasets. The altimeter data have been adjusted to be unbiased relative to the Church and White (2006) data in the period of overlap. The 90% confidence intervals are shown. [After Solomon et al. (2007, Fig. 5.13)].

runoff associated with decreases in groundwater storage, and increased precipitation over the ocean relative to evaporation. Movement of water substance from land to ocean further impacts sea level via gravitational self-attraction and loading (e.g., Mitrovica et al. 2009).

2) **Changes in density.** Water density changes are often referred to as the steric response and include both temperature (thermosteric) and salinity (halosteric) effects. Waters from land reservoirs that increase the mass of the ocean also reduce its salinity and density.
3) **Changes in geometry.** Relative land motions occur because of glacial isostatic adjustment (GIA), tectonic uplift or subsidence, sediment loading, and extraction of oil, gas, and water. These motions can change the coast line, local ocean bathymetry, and the relative position of tide gauges relative to the geoid.
4) **Changes in ocean circulation.** The ocean circulation varies regionally on a range of time scales and tends to be balanced geostrophically by the mass field. Part of the ocean circulation and respective sea level variability is due to the seasonal cycle in surface atmospheric winds and in the heat and freshwater fluxes at the ocean surface and from rivers. Therefore, correlations might be expected between the seasonal cycle of sea level and the seasonal cycle of storms. Here we assume that the seasonal cycle is not changing in time.
5) **High-frequency processes.** A number of processes affect sea level on submonthly time scales. These include synoptic weather and the short period tides. Storm surge associated with tropical and extratropical cyclones has clear and dramatic impacts on sea level on time scales of hours to days. In addition, day-to-day changes in surface atmospheric winds and pressure affect sea level on a continuum of intra-annual time scales. The isostatic response to atmospheric pressure, the so-called inverted barometer effect, may not hold at submonthly periods (Ponte 2006).

The regular rise and fall of sea level due to the solar and lunar astronomical tides is the most predictable component of sea level variability. The largest variations are on daily and monthly time scales. Seasonal and longer-term modulations are also predictable. The amplitude of the (equilibrium) annual tide ranges from 1 mm at the equator to 2 mm at the poles, and the semiannual tide is about 7 times larger (Egbert and Ray 2003). These, however, are small compared to daily and monthly tides and for simplicity are not included in our analysis.

In this work, with one exception, we will assume that the storm and tidal components do not change in the future. For storms we will analyze only the impact of the storm surge from tropical cyclones and, as described below, we use both the ''standard'' and warm sea surface temperature (WSST) catalogs as described by Dailey et al. (2009). The WSST catalog reflects the impacts on frequency and intensity of hurricane landfalls due to typical warm ocean conditions observed over the past century.

Secular trends in relative sea level can be estimated from tide gauge data. Two such estimates of the rate of sea level rise are used here. Both are based on monthly average tide gauge data with daily and subdaily tides filtered out. A simultaneous estimate of the seasonal cycle was also obtained but is ignored here. The first estimate was calculated by Hill et al. (2007) by correcting a global tide gauge dataset for the inverted barometer effect (Ponte 2006) and ocean circulations estimated from a dynamical model, and then fitting the remaining signal with a secular trend and a seasonal cycle. The tide gauge data in this case are from the Permanent Service for Mean Sea Level (PSMSL; http://www.pol.ac.uk/psmsl/psmsl_individual_stations.html) and cover a period of approximately 40 years. The 40-yr period matches the period of high-quality meteorological reanalysis beginning in 1958 that provided forcing fields to the ocean model used by Hill et al. (2007) to generate the ocean circulations. These estimates of the rate of sea level rise are referred to as the ''full model'' estimates here, and a scenario based on these estimates is referred to as a ''Full Scenario'' and is denoted simply as ''Full'' in table headings and figure legends. The second estimate was determined by a linear least squares fit to the National Oceanic and Atmospheric Administration (NOAA) tide gauge data (NOAA 2007), using the method of Zervas (2001), which includes a

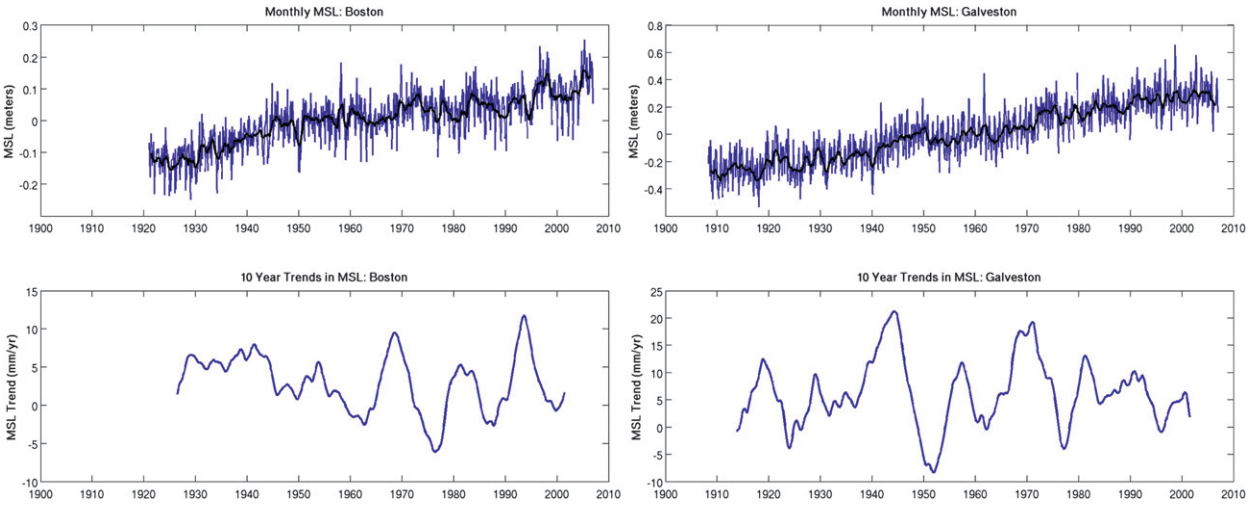


FIG. 2. Relative sea level for (left) Boston, MA, and (right) Galveston, TX, showing (top) the monthly mean (blue) and annual moving average (black) and (bottom) 10-yr trends of monthly mean sea level calculated using a sliding window. Data are from the Permanent Service for Mean Sea Level (PSMSL; http://www.pol.ac.uk/psmsl/).

secular trend and an annual cycle in fitting an autoregressive process to the monthly sea level data. According to Zervas (2001, Table 2) the average standard error of mean sea level trends determined in this way is ~0.5 mm $yr^{-1}$. These estimates are referred to as the "reduced model" estimates here, and a scenario based on these estimates is referred to as a "Reduced Scenario" and is denoted simply as "Reduced" in figure legends. (Note that we capitalize specific scenario names but not named estimates of sea level change.) The analysis by NOAA included 67 tide gauges along the U.S. Gulf and East Coasts, all with records of at least 30 years. (Of these, 46 have at least 50 years of data.)

A noteworthy result is that the difference in sea level rise between the two methods is coherent along the East Coast with smaller sea level rises north of approximately Washington, D.C., and larger sea level rises to the south in the Hill et al. (2007) analysis. In both cases the analysis provides an uncertainty estimate for the rate of sea level rise. Any processes not included in these estimates contribute to the uncertainty. The full model uses separate estimates of the ocean variability component, thereby eliminating one source of variability and increasing the variance explained in the overall fit. The reduced model uses the entire available record (in some cases more than 100 years), which serves to reduce the uncertainty of the slope estimate in the regression analysis. As a result, the uncertainty estimates of the full and reduced models are similar. Generally, at gauges where the ocean variability is significant and not a simple linear trend, the uncertainty of the full model will be less than the uncertainty of the reduced model. Similarly, where the historical tide gauge record is significantly longer than the 40 years used by Hill et al. (2007), the reduced model uncertainty will be less.

It should be noted that the interannual component of sea level variability is large, on the order of 10 mm $yr^{-1}$ with large temporal variability. For example, Fig. 2 shows the PSMSL monthly and annual mean data for Boston, Massachusetts, and Galveston, Texas, and 10-yr trends calculated from the monthly mean data. Note that a different vertical axis is used in each panel of Fig. 2. While the overall trend at Boston over the period of record from 1921 to 2006 is 2.6 mm $yr^{-1}$, there are substantial interannual and seasonal variations. The 10-yr trends (i.e., trends determined from overlapping 10-yr sequences) can be up to 4 times the magnitude of the long-term trends (as in the 1990s) and are even negative at times (as in the 1970s). At Galveston, the overall trend from 1908 to 2006 is 6.4 mm $yr^{-1}$. This is considerably higher than most of the trends seen for other U.S. stations and is only exceeded by Grand Isle, Louisiana, which has a rate of almost 10 mm $yr^{-1}$. At both Galveston and Grand Isle local oil and gas extraction make a significant contribution to the relative sea level rise (Morton et al. 2005). Again, 10-yr trends for Galveston are quite variable, ranging, in the extreme example of the 1940s and 1950s, from nearly +20 mm $yr^{-1}$ to nearly −10 mm $yr^{-1}$.

We use the uncertainties of the gauge estimates of the rate of sea level rise to determine the minimum and maximum rates of sea level rise that bracket the true sea level rise 95% of the time. These uncertainties reflect all sources of variability not included in the model. For example, variations shown in Fig. 2 cannot be captured by the reduced model but may be included in the full model

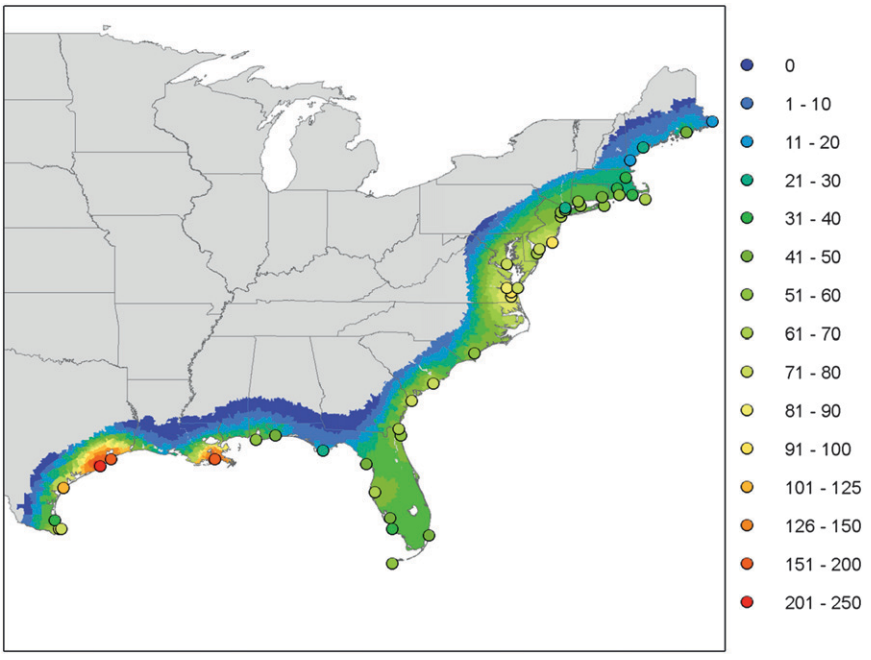


FIG. 3. Nominal 2030 projection of relative sea level rise (mm) based on the full model extrapolation of NOAA tide gauge records. Projected increases in sea level are color coded in the circle plotted at each tide gauge location. Gridded values, using the same color scale, were calculated as the weighted average of the tide gauge values, with weights inversely proportional to distance between the grid point and the tide gauge. Gridded values are plotted only in the coastal region approximately 160 km wide that includes all areas at risk from storm surge.

to the extent that these variations are caused by changes to the ocean circulation that are accurately represented by the dynamical ocean model in Hill et al. (2007). The set of minimum or maximum estimates of the rates of sea level rise at the gauges is used to estimate the change in risk associated with sea level rise as described below and in section 3. The levels of risk corresponding to the minimum and maximum estimates of sea level rise provide a confidence interval for the projected risks given in section 4. This confidence interval is different and probably smaller than a true 95% confidence interval for two reasons. First, simply using the slope uncertainty and extrapolating is not proper within the linear regression methodology. Second, if the climate is changing, the assumptions that we are modeling a stationary, equal variance process are invalid. Finally, we note that our confidence intervals for the sea level rise at individual stations are much smaller than the variability of some climate sea level projections based on climate models (Pachauri and Reisinger 2007).

To extrapolate sea level rise, we assume that the estimated past rates will persist into the future over the analysis period. In the experiments reported here, we convert the rate of sea level rise to an expected sea level change at each station for 2030. To quantify the error in this extrapolation we performed the following calculation. For the 10 NOAA tide gauge stations with records longer than 70 years, we *extrapolate* the record to 2008, using a least squares fit to annual average data prior to 1988, and compare to both the actual value *observed* in 2008 and the least squares fit *estimate* using all available data. The root-mean-square (rms) difference between observed and extrapolated is 25.0 mm (or 1.2 mm $yr^{-1}$) and between estimated and extrapolated is 18.0 mm (or 0.86 mm $yr^{-1}$). (For reference, the rms estimated sea level rise for all 67 NOAA tide gauge stations is 3.7 mm $yr^{-1}$.) This shows that half of the variance of the observed minus extrapolated difference is due to uncertainty in the slope and half is due to decadal and interannual variations. A fine grid of sea level increments for each future scenario is created by averaging the station values close to each grid point with weights inversely proportional to distance squared. To quantify the error in this interpolation we used the same procedure to interpolate to each NOAA tide gauge station location from surrounding stations. The rms difference, between interpolated and estimated sea level rise, for the 62 stations that have sufficiently close neighbor stations is ~0.84 mm $yr^{-1}$. The result for the Full Scenario is shown in Fig. 3. The changes in sea level over 20 years are estimated to be at most a few tenths of a meter. There are some notable geographical variations evident. The largest sea level rise occurs along

the Gulf Coast in the region centered on Louisiana, roughly from Freeport, Texas, to the end of the Mississippi Delta, except along the western Louisiana coast where there are no nearby tide gauges used in the Full Scenario. In this region, sea level rise is enhanced through a combination of sediment loading, subsidence due to oil and gas extraction, and erosion (Morton et al. 2005). Another region of enhanced sea level rise is found on the East Coast, peaking at Chesapeake Bay, where the forebulge that developed in front of the last glaciation is still relaxing back to its preglacial equilibrium (Calais et al. 2006). Differences between sea level increments in the Full and Reduced Scenarios are small, on the order of a centimeter, exceeding magnitudes of one or two millimeters only in areas where there were differences in the number or placement of tide gauges used in the analyses.

Our approach to extrapolating sea level rise is a conservative approach since the true sea level rise may be accelerating currently and this acceleration may increase in the future. For example, Church and White (2006) report improved fits for the global component by allowing for a change in slope or quadratic behavior in time. An alternative approach that might be taken is to replace the global component in the tide gauge rate of sea level rise with a more current estimate from the altimeter era. Cazenave and Nerem's (2004) altimeter-based estimate of the global component is $3.1 \pm 0.4$ mm yr$^{-1}$ for the period 1993–2003. (Before the adjustment for postglacial rebound their value is 2.8 mm yr$^{-1}$.) The $\pm 0.4$ mm yr$^{-1}$ value is probably an underestimate of the uncertainty, considering the possibility of unknown systematic errors. For comparison, the Church and White (2006) global reconstruction of the tide gauge record for the twentieth century gives a global estimate of the rate of sea level rise as $1.7 \pm 0.5$ mm yr$^{-1}$. While our approach is conservative for projecting sea level, we underestimate the uncertainty in our projections. That is, we are neglecting variability on decadal and shorter time scales, except for that due to storms. For example, ocean circulation decadal variability might give faster or slower rates or even negative rates of local sea level rise over 10–20-yr periods (as is evident in Fig. 2).

## 3. Modeling surge losses

The proprietary AIR hurricane catastrophe (CAT) model provides the framework to estimate the change in risk associated with sea level rise. Although this model has not been formally vetted in the scientific peer-reviewed literature to assess the model's individual components, it has been rigorously evaluated by the insurance industry, and because of its importance in risk management it has been reviewed by various regulatory bodies. As a part of this review process, technical details related to model implementation, input data sources, and supporting literature are publicly disclosed. Further, CAT models must ultimately demonstrate skill in predicting losses for hundreds of insurance companies with diverse portfolios and for all reasonable storm parameter combinations observed in U.S. landfalling hurricanes. Without an accurate representation of both the wind and surge hazards, the model would not be able to produce valid results for such a wide spectrum of risk. Further details describing the model and its validation are provided below and in appendix B.

The key element of the AIR hurricane model for this study is the storm surge module. This model component is a parametric, time-evolving storm surge simulator, which is based on a number of key storm parameters, including maximum wind speed, central pressure, size of the storm (radius of maximum winds), forward speed of the storm, and storm track (angle of attack against the coastline). These parameters all modulate the sea surface levels, especially to the right side of the storm (in the Northern Hemisphere) where the translation speed and the relative wind speed add to produce the largest wind stress and generally the largest surge heights. The storm parameters are taken from a catalog of $N$ years of simulated Atlantic tropical cyclones provided by a stochastic hurricane model. Here $N = 10\,000$, which is large enough to ensure that the results are sufficiently converged in the current study, where damage to all properties with no exclusions is determined. Much larger hurricane catalogs are required when applying the CAT model to the exposure of a single insurer. Losses are calculated for each storm in the catalog. Average annual losses are then estimated as the total loss for the entire catalog divided by $N$. The distribution of losses in the $N$ simulated years can also be estimated, and from this exceedance probabilities (or equivalently, losses corresponding to different return periods). So, for example, the 100-yr return period loss corresponds to the level of simulated loss from a single event that is expected to occur once in 100 years (i.e., the loss at the 0.99 level in the cumulative probability distribution).

The stochastic hurricane model hierarchically combines several probability distributions, which are empirically determined from the historical record. First, the number of storms in a given month is determined from probability distributions for the number of storms per year and the fraction of a year's storms that occur in each month. Information for each storm is then generated from probability distributions that are a function of location for genesis, intensification rate, track speed, and track direction. In addition, the probability distribution of the radius of maximum winds is conditioned on the storm intensity. The resulting catalog of simulated storms captures the natural variability of storm characteristics,

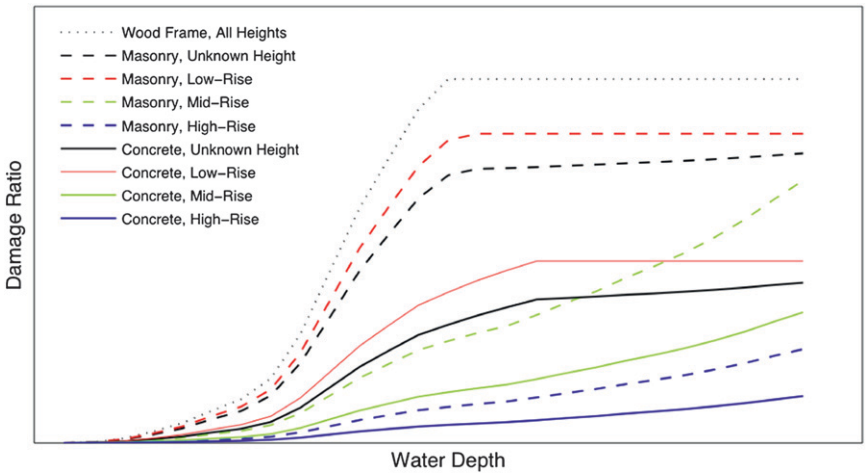


FIG. 4. AIR worldwide storm surge damage functions for different height and construction categories of general commercial property. Damage ratio is the average ratio of the repair cost to replacement value for properties subjected to a specific water depth.

including the space, time, frequency, and intensity characteristics. The 10 000-yr catalog used in this study contains approximately 19 000 hurricanes that make landfall along the U.S. coastline.

The parametric surge model also takes into account several local factors including the bathymetric profile, coastal geometry (e.g., surge amplification in bays), phase of the astronomical tide, land elevation, and terrain roughness. The latter two factors affect how the surge attenuates inland from the coastline. Bathymetry is critical in determining the peak surge at a given location (e.g., Irish et al. 2008) because the slope near the shore is a controlling factor in both wind and wave setup. In general, wind setup is greatest over a continental shelf with a mild slope (~1:10000) because the direct effect of wind stress on surge height is approximately proportional to the length and slope of the basin. On the other hand, wave setup is greatest over a steep-sloped shelf (~1:250) where friction has less time to act, resulting in taller breaking waves that then transfer more momentum from the waves to the water column. The surge model accounts for the local bathymetric profile using shoaling factors following Jelesnianski (1972).

This study makes use of the hazard output of the storm surge module, namely the peak surge height as a function of position. The surge height is interpolated to the location of each property in the property database, which will be referred to here as the Industry Exposure Database (IED). A civil engineering or "vulnerability" model then applies empirical-statistical parameterizations to determine the fraction of the total property value that is damaged as a function of surge height. These parameterizations or "damage functions" are specified differently for each construction type (e.g., Sill and Kozlowski 1997; Unanwa et al. 2000; Rosowsky and Ellingwood 2002; Lee and Rosowsky 2005). The IED includes detailed information on insured properties. Losses to all individual commercial and residential real estate properties are then aggregated over zip codes, states, and finally regions for each storm and for each year. These losses are termed "ground up" losses. The term "ground up losses" is used because our calculations do not include losses to so-called "in-ground" infrastructure, including roadways, utility networks, pipelines, urban transit facilities, and other assets that might be present in high concentrations in urban areas and may in fact be insured.

While the intensity parameter used in the storm surge module of the AIR model is water depth, the nature of damage from storm surge is quite different from the damage caused by standing water (e.g., Kennedy et al. 2010). Therefore, the model's damage functions take into account the momentum as well as the depth of the water. The Federal Emergency Management Agency (FEMA) and the Army Corps of Engineers observational data were used in the development of the surge damage functions. The damage functions have been validated with AIR postdisaster survey data as well as with industry and company loss experience data.

Damage from storm surge is modeled as a function of building construction type, height, and occupancy. Building height is a significant variable in surge damage estimation as upper stories are less vulnerable. Both content damage and loss of use (or time element damage) are estimated. For the time element, the model estimates the effective downtime before the facility is restored or usable. Figure 4 shows the shapes of the functions used in the AIR model for the class of general commercial properties for different height categories

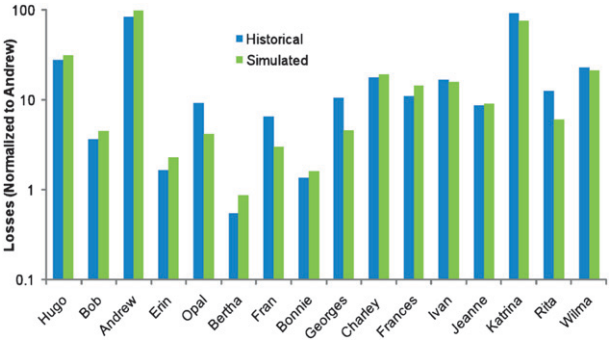


FIG. 5. Actual vs simulated losses for U.S. landfalling hurricanes from 1989 to 2005. All losses were adjusted for inflation and then normalized to the historical losses of Hurricane Andrew (1992).

and construction types. This figure clearly demonstrates the complex, nonlinear nature of these storm surge damage functions.

Since the primary use of the AIR hurricane model is to provide loss estimates to insurance companies, this is ultimately the metric used to validate the model. Of course, modeled wind speeds and surge heights must also validate well in order to produce accurate loss estimates for landfalling hurricanes. (Additional validation is provided in appendix B.) The AIR model has been validated extensively using actual loss data and has a long and impressive record of providing reliable, credible estimates of property loss. AIR has compiled an extensive database of 20 years' worth of claims data for historical U.S. hurricanes from several major client companies. Further validation is undertaken after each damage survey, which AIR has conducted for every U.S. landfalling hurricane since Hurricane Hugo in 1989. Figure 5 compares actual and simulated insured losses for hurricanes that made landfall in the United States between 1998 and 2005. The simulated losses compare well to the actual losses. Since the loss estimates are dependent on the accuracy of the meteorological components of the model, the skill shown in Fig. 5 demonstrates the internal consistency of the underlying components of the model and the validity of the overall model for this purpose.

To include sea level rise in the surge model, we subtract it from the current land elevations. For example, the land elevation used in the Full Scenario is given by the difference of Fig. 6 minus Fig. 3. Low-lying areas in Fig. 6 (say, areas at elevations below 3 m) are already sensitive to surge. In our projection for 2030 conditions, they will be even lower relative to sea level. We will focus on these regions in our analysis (section 4). Note that several low-lying areas are within the regions where the largest rises in the sea level are expected to occur, as described in section 2. These include the low-lying areas along the coast of Louisiana, eastern Texas, the eastern shore of the Chesapeake Bay, and the area centered around Cape Hatteras. South Florida, including all the areas around Florida Bay and the Everglades, is also a low-lying region of considerable interest. (Place names referred to in the text are plotted in Fig. 6.)

Calculations with current conditions (i.e., the standard catalog and the current land elevation) provide the baseline estimate of risk. To obtain the changes in surge risk, the adjusted elevation is used. The 95% confidence interval of the rate of sea level rise is propagated through the CAT model by using the upper and lower bounds to adjust the land elevation. Also, the sensitivity of the surge risk to possible changes in storm and landfall characteristics associated with warmer sea surface temperatures is assessed by using another 10 000-yr stochastic catalog. The WSST catalog has been developed to specifically reflect storm characteristics that are associated with warmer than normal sea surface temperature conditions (Dailey et al. 2009).

In making use of the WSST catalog, this study tests the sensitivity of U.S. storm surge risk to conditions observed under warmer than average SSTs, which serves as a partial analog for a potentially warmer ocean climate in the next 20 years. However, it must be kept in mind that there are many ways to project future tropical cyclone activity and all such projections currently have large error bars (Knutson et al. 2010). First, in terms of observed trends, some scientists argue that the series of observed warm SST anomalies in the Atlantic since the mid-1990s is a temporary episode due to a natural cycle (e.g., Landsea 2005; Vecchi and Knutson 2008), and others argue that the warming trend is permanent for the foreseeable future (e.g., Mann et al. 2007). Other factors related to hurricane activity, notably El Niño (e.g., Saunders et al. 2000; Donnelly and Woodruff 2007) and aerosols including Sahara dust (e.g., Dunion and Velden 2004; Mann and Emanuel 2006), may also have significant trends. For example, there may be a trend in the relative frequency of the different types of El Niño (Kug et al. 2009), and these types likely have different relationships with Atlantic tropical cyclone activity (e.g., Hye-Mi et al. 2009). Second, modeling studies that attempt to link observed, hypothesized, or projected changes in the global climate to future hurricane risk (e.g., Bender et al. 2010) must account for biases and uncertainty in projections of factors that impact tropical cyclone activity, such as global and regional SSTs, vertical wind shear, and tropical troposphere thermodynamic states (Sabbatelli and Mann 2007). Additional uncertainties can be introduced by the complexity of how these environmental factors affect tropical storms (Emanuel 2005; Swanson 2008) and the difficulty of simulating the multiscale physical and dynamical processes of tropical cyclones (Bender et al. 2007). In part because

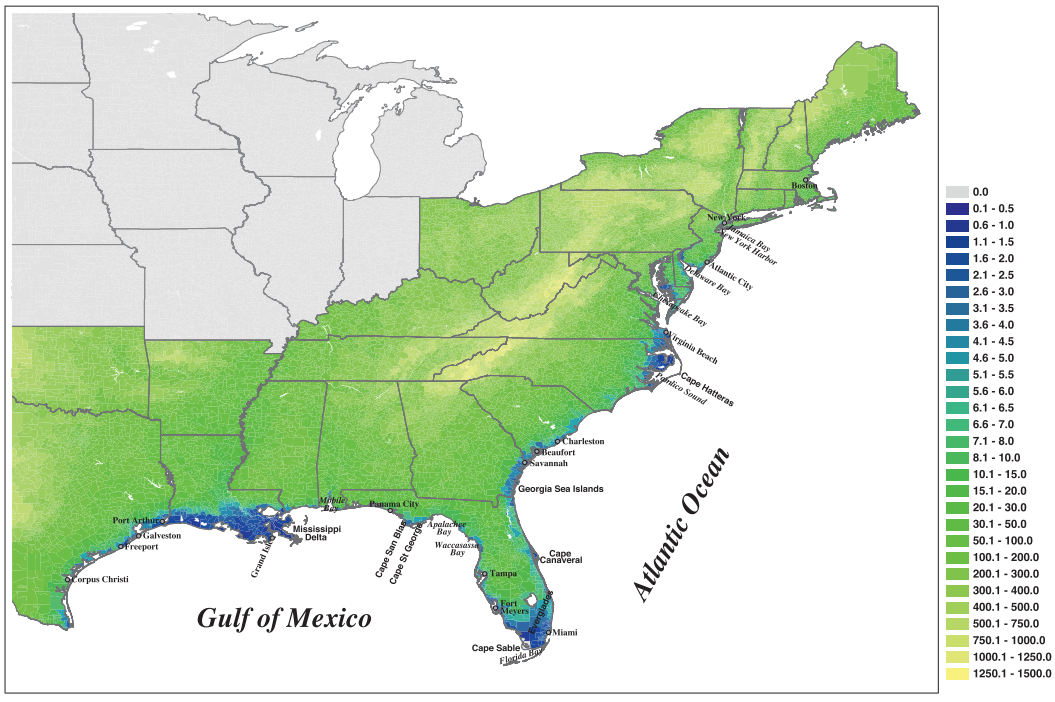


FIG. 6. Representation of topography in the surge model. Land surface elevation in meters for the U.S. Gulf and East Coasts is indicated by the color scale.

climate change scenarios contain wide-ranging estimates of changes to these parameters (Knutson et al. 2010), it is currently not possible to accurately quantify future hurricane risk with high statistical confidence. Significantly more research will be required to resolve this debate (e.g., Shepherd and Knutson 2007), especially in projecting climate conditions toward the end of the twenty-first century.

In this study, to explore the implications of a changing climate to hurricane and storm surge risk over the next 20 years, we avoid some of the above sources of uncertainty by using the WSST catalog. The collection of hurricane events in the WSST catalog represents the response of regional U.S. landfall risk to observed warmer than average Atlantic SSTs. Using over 100 years of historical data, Dailey et al. (2009) found that warm Atlantic SST anomalies, which periodically occurred in approximately 50% of the historical record, have a statistically significant influence on U.S. hurricane risk. This influence includes changes to hurricane intensity, frequency, track, and formation regions. In contrast to other studies that take into account many climate factors (e.g., Knutson et al. 2010; Bender et al. 2010), Dailey et al. (2009) consider only how tropical cyclone activity (and implicitly other factors) historically varies with Atlantic SSTs. Although this partial analog approach does not account for all processes that may change in the future, it has the advantage of providing finescale sensitivities. Note that risk measures conditioned on warm SSTs assume that other important variables are consistent with historically warm SST periods. In particular, the WSST catalog used in this study does not assume neutral wind shear conditions but rather wind shear conditions that have been observed under warmer than average ocean conditions.

Dailey et al. (2009) showed that during years in which SSTs are warmer than the long-term average, the U.S. Gulf and East Coasts experience more frequent tropical cyclone landfalls. The findings further indicate that tropical cyclone intensity at landfall is also affected by warm ocean conditions and the effect varies by region. In particular, the Gulf Coast is likely to experience more frequent landfalls of tropical storms, but little increase in the number of hurricane landfalls. The pattern is different for the southeast, which is likely to experience more frequent storms of hurricane strength. In the northeast, the relationship between warm SSTs and hurricane landfalls is too weak to draw a clear conclusion. Overall, the increase in the mean frequency between the WSST catalog and standard catalog is modest, generally between 5% and 10%.

The calculation described in this section is, as mentioned in the introduction, a preliminary sensitivity study. It differs from a realistic projection of loss in several important aspects. First, we use the current coastline and property database (IED). In the future, property along the coast will change in terms of density, value, and construction

TABLE 1. List of experiments. For each scenario the hurricane catalog and method of projecting sea level are given.

| Scenario | Catalog | Sea level projection |
|---|---|---|
| Baseline | Standard | None |
| Full | Standard | Full model estimate |
| Full LB | Standard | Full model lower bound |
| Full UB | Standard | Full model upper bound |
| Reduced | Standard | Reduced model estimate |
| Reduced LB | Standard | Reduced model lower bound |
| Reduced UB | Standard | Reduced model upper bound |
| Full + WSST | WSST | Full model estimate |
| Full + WSST LB | WSST | Full model lower bound |
| Full + WSST UB | WSST | Full model upper bound |
| Reduced + WSST | WSST | Reduced model estimate |
| Reduced + WSST LB | WSST | Reduced model lower bound |
| Reduced + WSST UB | WSST | Reduced model upper bound |

techniques. Further, erosional processes are expected to alter the coastline as sea level rises. For example, if sea level rises slowly enough, dune systems, marshes, and other coastal ecosystems respond by retreating inland. If sea level rises too fast, these ecosystems will become inundated. These changes are not included here. Second, as discussed above, a number of studies have examined how tropical cyclone frequency and intensity might change as climate changes in the future. Here, however, except for the warm SST sensitivity experiment, storm characteristics are held constant. Finally, our extrapolation of sea level is conservative. Apart from extreme possibilities such as an abrupt and catastrophic collapse of the Greenland Ice Sheet in the manner described in Pfeffer et al. (2008), decadal ocean circulation anomalies can imply substantially different decadal sea level rates, as seen in Fig. 2, and therefore larger uncertainties than what we estimate here.

## 4. Projected losses and discussion

We compare results from calculating ground up loss according to several scenarios (see Table 1). The Baseline Scenario includes current sea level and the standard catalog of 10 000 years of stochastically simulated hurricanes. The Full Scenario includes the full model estimate of sea level for 2030 and the standard catalog. The Reduced Scenario is like the Full Scenario but uses the reduced model estimate of sea level for 2030. Two additional scenarios, denoted Full + WSST and Reduced + WSST, replace the standard catalog with the WSST catalog of 10 000 years of stochastically simulated hurricanes. For each scenario, except for the Baseline Scenario, we also calculated losses that correspond to the 95% confidence interval upper bound (UB) and lower bound (LB) estimates of sea level rise. For example, the Full + WSST UB Scenario includes the upper bound of the 95% confidence interval for sea level rise from the full model estimates along with the WSST catalog. This scenario corresponds to an extreme projection with both large increases in sea level and hurricane activity and is examined in some detail in what follows.

TABLE 2. Total aggregate losses (in USBS; i.e., all dollar amounts are normalized by the AAL for the U.S. Baseline Scenario) and percent difference from Baseline for the Full and Full + WSST Scenarios for the entire U.S. Gulf and East Coasts (US). Total aggregate US losses for the Baseline (BL) Scenario are listed for comparison. Losses are given for the aggregate annual average loss (AAL), the 50-yr return period loss (50-yr RP), and the 100-year return period loss (100-yr RP). The 50-yr (100-yr) loss is the loss that has a 2% (1%) probability of occurring or being exceeded in any year. The 95% confidence interval upper and lower bound (UB, LB) for each projected loss are given.

| | | BL | Full | | | Full + WSST | | |
|---|---|---|---|---|---|---|---|---|
| Type | Units | Loss | LB | Loss | UB | LB | Loss | UB |
| AAL | USBS | 1.00 | 1.07 | 1.08 | 1.09 | 1.18 | 1.19 | 1.20 |
| | % | | 6.95 | 7.84 | 8.75 | 17.61 | 18.61 | 19.62 |
| 50-yr RP | USBS | 6.23 | 6.46 | 6.49 | 6.52 | 6.64 | 6.65 | 6.67 |
| | % | | 3.70 | 4.21 | 4.64 | 6.55 | 6.77 | 6.98 |
| 100-yr RP | USBS | 7.50 | 7.69 | 7.72 | 7.75 | 7.78 | 7.81 | 7.84 |
| | % | | 2.48 | 2.97 | 3.36 | 3.69 | 4.07 | 4.55 |

Aggregate losses for the entire U.S. Gulf and East Coasts (hereafter denoted US when describing losses to the entire region) are displayed in Table 2 for the Baseline, Full, and Full + WSST Scenarios. Results for the Reduced and Reduced + WSST Scenarios are not shown here since these are so similar to the results for the corresponding Full and Full + WSST Scenarios. The table shows the average annual loss (AAL), the 50-yr return period loss (50-yr RP), and the 100-yr return period loss (100-yr RP). These estimated losses are calculated as described in section 3. As noted in the introduction, we do not presume to predict future property values. Therefore, only the relative variations are meaningful for comparison with future scenarios. Further, because data on surge losses are limited, surge risk itself is not well documented. Consequently, although our model is well calibrated for application to insurer exposure, actual dollar losses calculated here are subject to large error bars. In what follows relative values and percentage changes are considered to be the most trustworthy metric. Further considering the business model and underwriting practices of the insurance industry, percentage change in risk is arguably the most relevant risk metric for insurers. Accordingly, here and in what follows we normalize all dollar amounts by the AAL for the U.S. Baseline Scenario. We define this value to be 1 USBS. For the Baseline Scenario, the AAL is thus 1 USBS, so once in 50 years the expected loss will exceed 6.23 USBS, and once in 100 years the expected loss will exceed 7.50 USBS. For the Full Scenario, the AAL is $1.08 \pm 0.01$ USBS, an increase of 8% relative to Baseline,

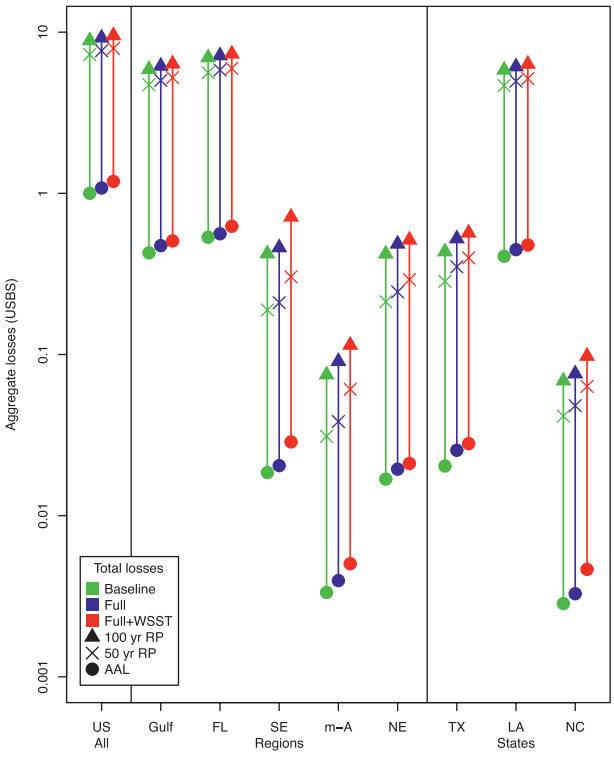


FIG. 7. Total aggregate losses (in USBS; i.e., dollar amounts normalized by the AAL for the U.S. Baseline Scenario, plotted on a log scale) for the Baseline (green), Full (blue), and Full + WSST (red) Scenarios for the U.S. Gulf and East Coasts (US), for US divided into several regions, and for three additional key states. (Abbreviations are defined in the text.) A different color (noted above) is used for each scenario, with the different scenarios plotted at different horizontal offsets to avoid overlap. For each region or state, a different symbol is plotted for the 100-yr return period loss (100-yr RP), the 50-yr return period loss (50-yr RP), and the annual aggregate loss (AAL). These three symbols are connected by a vertical line.

while for the Full + WSST Scenario the AAL is 1.19 ± 0.01, an increase of 19% relative to Baseline. For the more extreme events, the percentage increases in risk are smaller: less than half (3% versus 8%) for the 100-yr return period loss under the Full Scenario.

Figure 7 graphically shows a subset of the information in Table 2 for the United States and for other regions and a number of states. Expected losses (in USBS) range over several orders of magnitude and thus are plotted on a log scale. The regions dividing the United States are the Gulf (Texas, Louisiana, Mississippi, Alabama), Florida (FL), the Southeast (SE; Georgia, South Carolina, North Carolina), the mid-Atlantic (m-A; Virginia, Delaware, Maryland, Pennsylvania), and the Northeast (NE; New Jersey, New York, Connecticut, Rhode Island, Massachusetts, New Hampshire, Vermont, Maine). Losses for three key states—Texas (TX), Louisiana (LA), and North Carolina (NC)—are displayed separately as well. Values from the columns labeled "Loss" in Table 2 are plotted on the left side of Fig. 7. For example, the three green symbols on the far left correspond to the Baseline estimated losses quoted above. In all cases, expected losses increase as sea level rises and as hurricane landfall activity increases. Expected losses in each of Louisiana and Florida are very large, with losses of roughly 5 USBS to be expected every few decades. Most of the expected Gulf losses from surge occur in Louisiana. For the Southeast, North Carolina, and the mid-Atlantic, losses are much greater for the Full + WSST Scenario than for the Full Scenario. This result is generally consistent with the findings of Dailey et al. (2009; see their Fig. 6) that indicate that for landfalling hurricane-strength storms the greatest sensitivity to SST is along the East Coast.

To focus on the differences relative to the Baseline Scenario, Fig. 8 displays the differences in both USBS and percent, in estimated losses with respect to the Baseline Scenario. The differences are aggregated as in Fig. 7 (blue corresponds to the standard catalog and red to the WSST catalog), but here the results for both the Full and Reduced Scenarios are plotted. Again, the increases due to the WSST catalog are much greater for the Southeast and the mid-Atlantic regions, including North Carolina. Dailey et al. (2009) found that under warm SST conditions, storm genesis marginally favors Cape Verde–type storms that form farther east relative to average SST conditions. In addition, the location and strength of the Atlantic subtropical high during extended periods of elevated SSTs may favor steering these storms into the open Atlantic and mid-Atlantic region (Dailey et al. 2009; see their Fig. 13). The greatest increases for Louisiana and Florida relative to the Baseline Scenario are as much as 0.07 and 0.09 USBS, respectively, on an annual basis and up to 0.48 USBS every few decades. As a percent of the Baseline Scenario results, changes for Louisiana and Florida are small, 5% to 20% for the AAL, and no more than 12% for the 50- and 100-yr return period losses. The greatest percent increases—roughly 100%—occur for the mid-Atlantic region for the 50-yr return period loss. Uncertainties for North Carolina and the mid-Atlantic region are noticeably greater for the Reduced Scenarios.

We now examine how surge risk varies locally. Figure 9 shows the Baseline Scenario ground up loss cost along the coast of Florida due to storm surge. The ground up loss cost is the expected annual loss ratio, often expressed in dollars of loss per thousand dollars of property value. Most of the Florida coastline is vulnerable to hurricane storm surge. Areas at greatest proportional risk are on the southern Gulf coast of Florida, notably from Fort Myers southward toward Cape Sable. Values displayed in

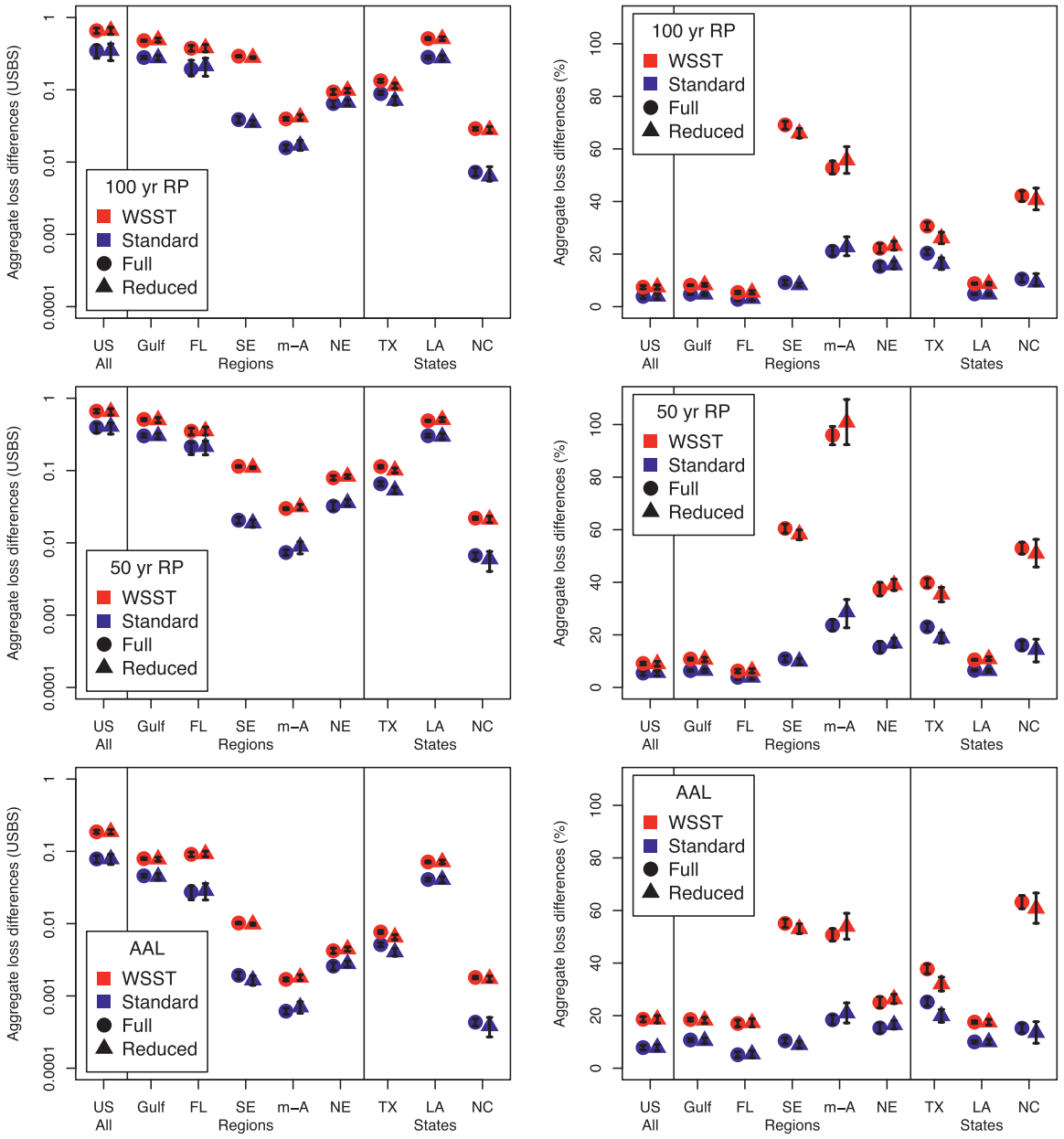


FIG. 8. Aggregate loss differences (in USBS on a log scale on the left and in percent on a linear scale on the right). A different symbol is used for the Full (○) and Reduced (△) estimates and different colors for the Standard (blue) and WSST (red) Catalogs for the (top) 100-yr RP, (middle) 50-yr RP, and (bottom) AAL. The Full and Reduced cases are plotted slightly to the left and to the right to avoid overlap. The 95% probability bounds are plotted on top of each symbol. In many cases these bounds are smaller than the symbol. NB: This uncertainty is due only to the uncertainty in the estimated slope of sea level rise.

this figure are normalized by the total value and do not highlight areas where the greatest aggregate losses are expected to occur. Even small rates of risk can aggregate to large values in metropolitan areas such as Miami and Tampa or in regions of wealth such as the barrier island beaches along the east coast of Florida from Miami northward to Cape Canaveral. Note that in the latter area, it is only property along the barrier beaches that is at risk to significant storm surge.

For the most part, the ground up loss costs for the other scenarios look similar to the Baseline Scenario and are not shown. Instead we present the difference from the Baseline Scenario in loss cost or in percent. Figure 10 shows the increase in ground up loss cost relative to the Baseline

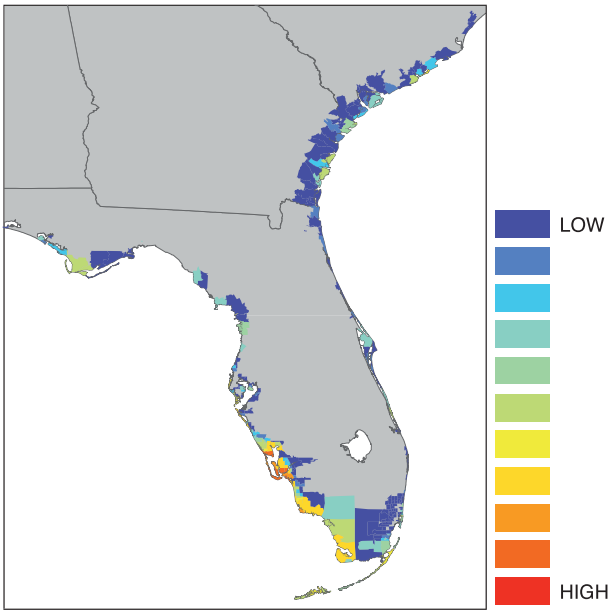


FIG. 9. The Baseline Scenario ground up loss cost ($/1000) along the Florida Coast by zip code. Only losses due to tropical cyclone surge damage are included. The ground up loss cost is the expected annual loss in dollars per thousand dollars of property. Values are based on current sea level using the standard catalog of 10 000 years of simulated tropical cyclones. The color scale from deep blue to dark red indicates increasing loss costs on a geometric scale with the maximum value doubling from hue to hue. As noted in the text, numeric values are not given because only the relative variations are meaningful for comparison with future scenarios. Areas with no expected surge losses are light gray.

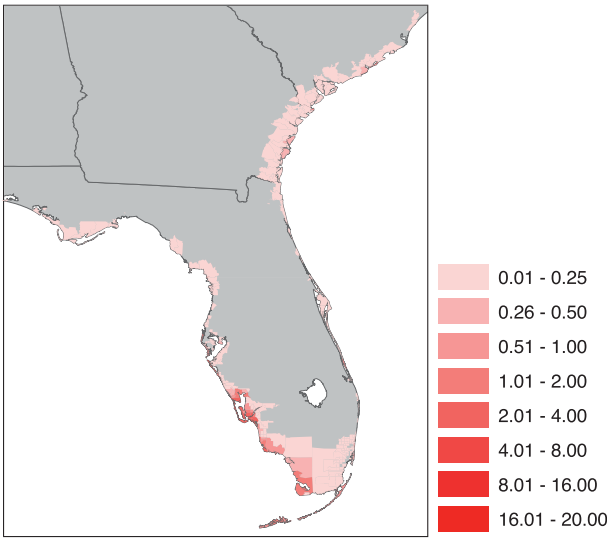


FIG. 10. The increase ($/1000) in ground up loss cost relative to the Baseline Scenario along the Florida coast for the Full Scenario. The Full Scenario extrapolates the full model estimates of sea level rise to 2030 and uses the Standard Catalog. The color scale from light pink to dark red indicates increasing loss cost differences. Areas with no expected surge losses in 2030 are light gray.

Scenario along the Florida Coast for the Full Scenario. The pattern of increase is qualitatively similar to the Baseline Scenario in that the areas of largest loss cost on the south Gulf coast of Florida are also areas of the largest increase. However, the similarity apparent to the eye does not hold up to quantitative analysis. Figure 11 shows the percentage change in ground up loss cost relative to the Baseline Scenario for this case. Here, the most noticeable percentage increase occurs at Waccasassa Bay (north of Tampa Bay and south of Apalachee Bay), an area with relatively small Baseline risk. In fact, percentage increases are relatively small in just those areas where the loss cost differences were greatest. An explanation of this phenomenon is offered in section 5 based on the shape of typical property damage functions.

The change in loss cost for two extreme projections relative to the Baseline Scenario are displayed in Fig. 12. The format is the same as in Fig. 10, but here the results for the Full + WSST UB and Reduced + WSST UB Scenarios are shown. The patterns in all three plots have a similar shape, but in both WSST Scenarios the increases in loss cost are significantly larger. The results for the two WSST Scenarios are similar. The increases in risk are largest around Cape San Bias and Cape St. George (between Panama City and Apalachee Bay), along the southwest coast of Florida, south of Miami, and along the Georgia and South Carolina coasts, from the Sea Islands to Savannah to Charleston. The same change in loss cost is presented as a percentage in Fig. 13 (cf. Fig. 11, which is in the same format). Percentage changes all increased somewhat, with the largest increase along the South Carolina coast from Beaufort to Charleston.

Figure 14 shows the Baseline ground up loss cost along the Gulf Coast, in the same format as Fig. 9. The vulnerability of the Gulf Coast to surge is very large from Galveston Bay in Texas all across Louisiana to Biloxi, Mississippi, with additional ''hot'' spots near Freeport and Corpus Christi, Texas. This vulnerability is extreme in the Mississippi Delta area and around Port Arthur, Texas. Note that the western edge of Mobile Bay is also at risk to storm surge far inland from the Gulf of Mexico proper because the shape and shoaling of Mobile Bay focuses storm surge, the western shore has lower elevations, and approaching storms often have an easterly component. Changes in loss cost for the same three scenarios discussed for Florida are shown in Fig. 15. Again the shape, as opposed to the amplitude, of the pattern of change is similar. For the most part the pattern is similar to the Baseline loss cost, as was the case for Florida. The Reduced + WSST UB Scenario has the largest increases, followed closely by the Full + WSST UB Scenario and then by the Full Scenario. Compared to what we observed

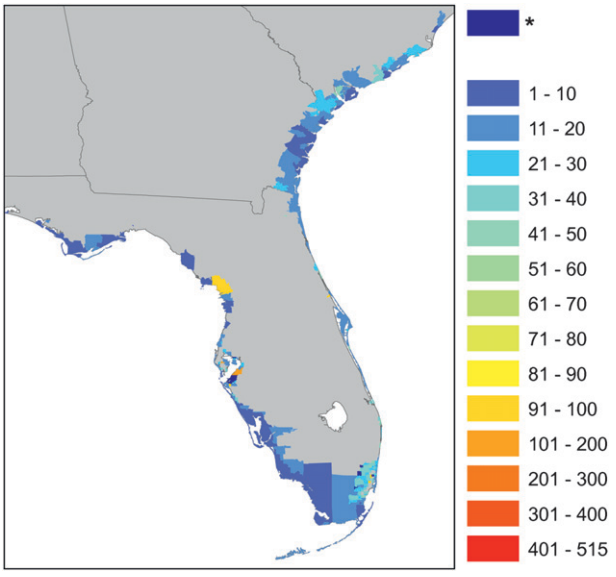


FIG. 11. The percentage change in ground up loss cost relative to the Baseline Scenario along the Florida coast for the Full Scenario. The percentage change is relative to current conditions (i.e., a 100% change corresponds to a doubling of the estimated loss). Note that some of the areas showing the largest percentage increases are areas that currently have very small expected surge losses. Areas with no expected surge losses in 2030 are light gray and areas that are dark blue (identified by the asterisk in the legend) are new areas of impact (i.e., these areas experience no surge loss in the Baseline Scenario, but do in the Full Scenario).

for Florida, results for the three scenarios agree more closely. Note that the loss cost for the Mississippi Delta region is increased substantially. This is an area expected to experience the greatest sea level rise, and it is an area already at high risk. However, in terms of percentages (Fig. 16), the changes are largest where the Baseline Scenario loss cost is smallest. This behavior was also seen along the Florida coast.

We note that risks along the coast of Mississippi appear small compared to recent experience because we model surge losses at the zip code level (see appendix B). As indicated by the gray shading in the figures, some regions located directly on the coastline (or very near the coast) do not experience surge loss. This result can occur for two reasons. First, this could be a manifestation of historic storm frequency at this location, storm strength, or other parameters governing surge at a given location (e.g., regions less susceptible to intense and frequent hurricane landfalls could potentially have no surge loss). Second—and this is the reason for the lack of risk in Mississippi—characteristics of each zip code (e.g., elevation) are determined based on the location of the population-weighted centroid of the zip code. For some zip codes, the centroid may be located very near the shoreline and for others it may be located relatively far inland and in a region of higher elevation. It is this second case that limits potential surge loss for a zip code. In future studies a finer grid should be used.

Figure 17 shows the Baseline ground up loss cost along the mid-Atlantic coast. The greatest vulnerability to storm surge in this region is centered on Cape Hatteras, from the southern reaches of the Pamlico Sound to Virginia Beach. Additional areas at risk are the eastern shores of the Chesapeake and Delaware Bays. Again, as with Mobile Bay, the shape and shoaling of these bays can focus storm surge, but in this region the many storms will have begun to recurve so the typical angle of attack has an eastward component, and the eastern shores have lower elevations than the western shores. Relatively minor surge risk exists for Atlantic City, New Jersey, and New York Harbor, especially Jamaica Bay. Of course, these qualifiers—greatest, minor, etc.—are for the relative risk in terms of loss cost. The huge property values in New York City compared to Cape Hatteras mean that actual total risk may be much greater in a New York zip code with a relatively small loss cost. Changes in loss cost for the same three scenarios discussed for Florida and the Gulf are shown in Fig. 18. Here, increases in loss cost for the two WSST Scenarios are very similar and both are considerably larger than for the Full Scenario. This is especially evident in terms of percentages. In Fig. 19, in the region around Cape Hatteras, but also in the Delaware Bay, both in the upper reaches of the bay and near its entrance at Cape May, many localities have increases in risk approaching 100%. Note that for the WSST Scenarios, in the Cape Hatteras region, in contrast to the other results of this study, localities currently at high risk also experiences the greatest increase in risk. As mentioned earlier, this result is generally consistent with the findings of Dailey et al. (2009).

## 5. Summary and concluding remarks

The AIR hurricane CAT model is used to estimate the sensitivity of storm surge risk to sea level rise. For this purpose we reduced land elevations used in the storm surge module of the CAT model by amounts equal to projected sea level increases. We compared the results of several future scenarios to a Baseline Scenario corresponding to current conditions. Note that the only difference between scenarios is the sea level increase and the hurricane catalog used. All other factors are held fixed. In particular, assumptions about the current coast line, land use, property values, and construction methods are unchanged. In each case, we calculated property value losses for the current property inventory for 10 000 simulated years of tropical storms. Only losses due to storm surge were calculated (i.e., losses due to wind or rain were not

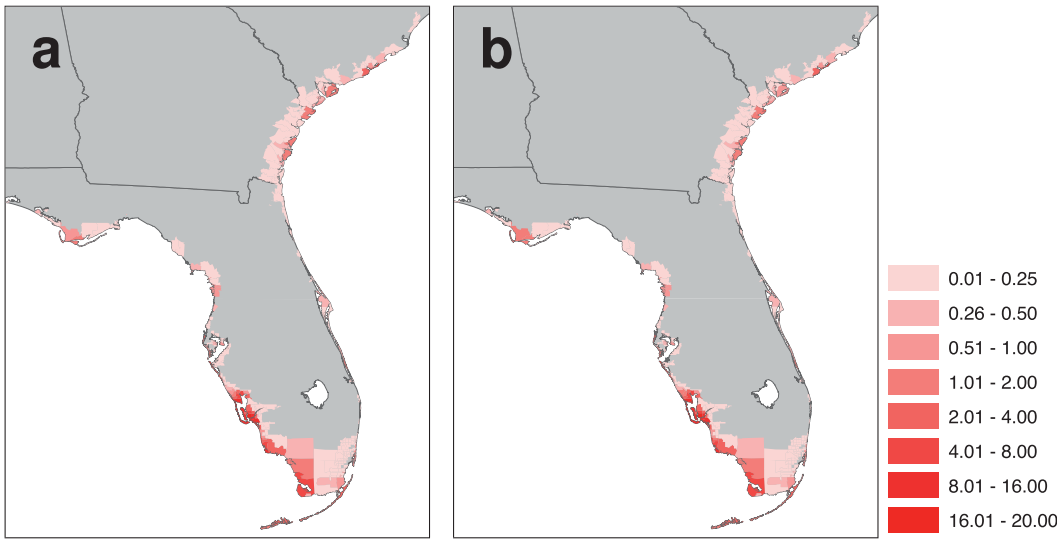


FIG. 12. As in Fig. 10, but for the increase ($/1000) in ground up loss cost relative to the Baseline Scenario along the Florida coast for the (a) Full + WSST and (b) Reduced + WSST upper bound (UB) Scenarios. The Full + WSST UB Scenario extrapolates the upper bound of the full model estimates of sea level rise to 2030 and uses the WSST catalog. (There is a 2.5% probability that sea level rise would exceed the upper bound.)

included). The losses for individual properties were then aggregated by zip code, by state, and by region. When normalized by the total property value (aggregated for each zip code), these losses were expressed as the ground up loss cost, which is the expected loss in dollars per thousand of dollars of value in the property inventory.

The Baseline Scenario results were compared to the results from two different estimates of sea level rise and two different stochastic hurricane catalogs. The estimates of sea level rise came from the work of Hill et al. (2007), based on combining model simulations with tide gauge data over a 40-yr period, and from data from NOAA (2007), based on a simple linear regression of all available tide gauge data. These estimates of sea level rise were used in the Full and Reduced Scenarios, respectively. The hurricane catalogs are the standard and warm SST (WSST) AIR catalogs. The WSST catalog was developed following the findings of Dailey et al. (2009). In addition, 95%

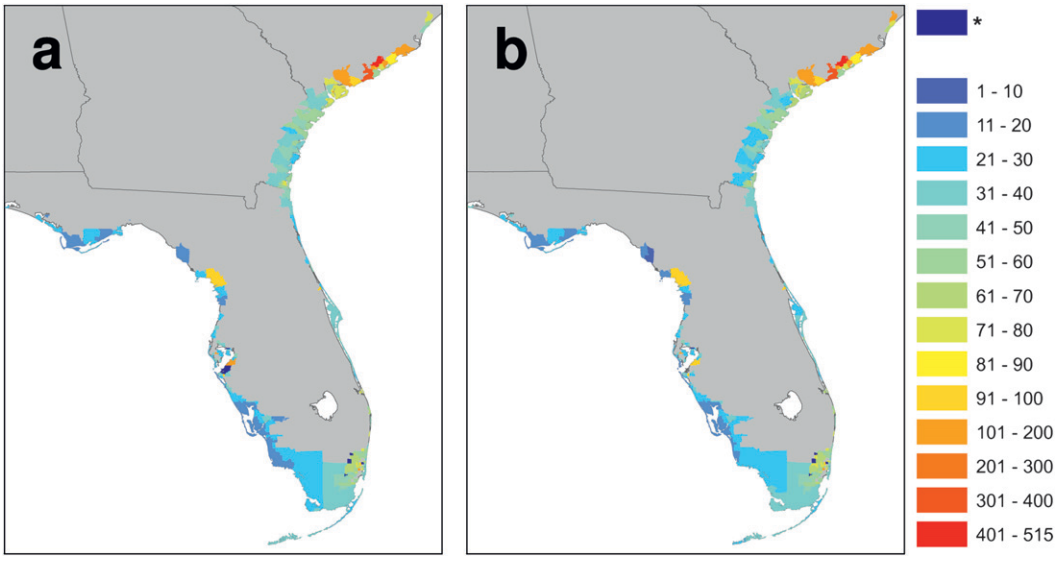


FIG. 13. As in Fig. 11, but for the percentage change in ground up loss cost relative to the Baseline Scenario along the Florida coast for the (a) Full + WSST UB and (b) Reduced + WSST UB Scenarios. (There is a 2.5% probability that sea level rise would exceed the upper bound.)

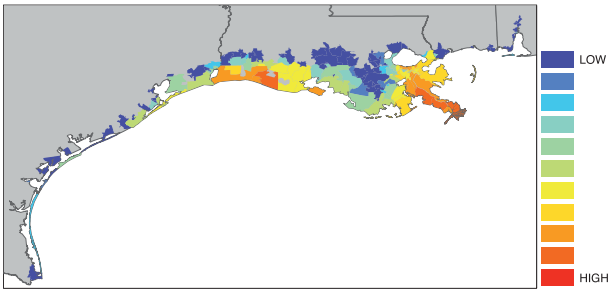


FIG. 14. As in Fig. 9, but for the Baseline Scenario ground up loss cost ($/1000) along the Gulf Coast.

confidence bounds on the rate of sea level rise at each tide gauge were propagated through the experimental setup to provide upper and lower bound (UB and LB) scenarios.

We examined the Baseline Scenario results and compared the Baseline Scenario results to results from the scenarios defined above. We find the following:

- In all cases expected losses increase as sea level rises and as hurricane landfall activity increases.
- Baseline expected average annual loss (AAL) for the entire U. S. Gulf and East Coasts (US) is 1 USBS. Single event losses are expected to exceed 6.23 USBS every 50 years.
- In 2030, for the full model estimate, US AAL is expected to increase by 8% if tropical storm activity does not change and by 19% if tropical storm activity is similar to that of the WSST catalog (i.e., similar to that of recent years with warmer than normal SST). Percentage increases in losses for the 50- and 100-yr return periods (i.e., the 2% and 1% exceedance probability values) are less than these values.
- For the southeast and mid-Atlantic coasts, losses for the WSST Scenarios are much greater than for the Standard Scenarios. This result is generally consistent with the findings of Dailey et al. (2009) that, for landfalling hurricane-strength storms, the greatest sensitivity to SST is along the southeast coast.
- On a regional or state basis, areas such as Louisiana and Florida that already have the largest dollar losses also have the largest projected increases in dollar losses, but on a percentage basis the regions or states with smaller Baseline Scenario losses have the largest projected

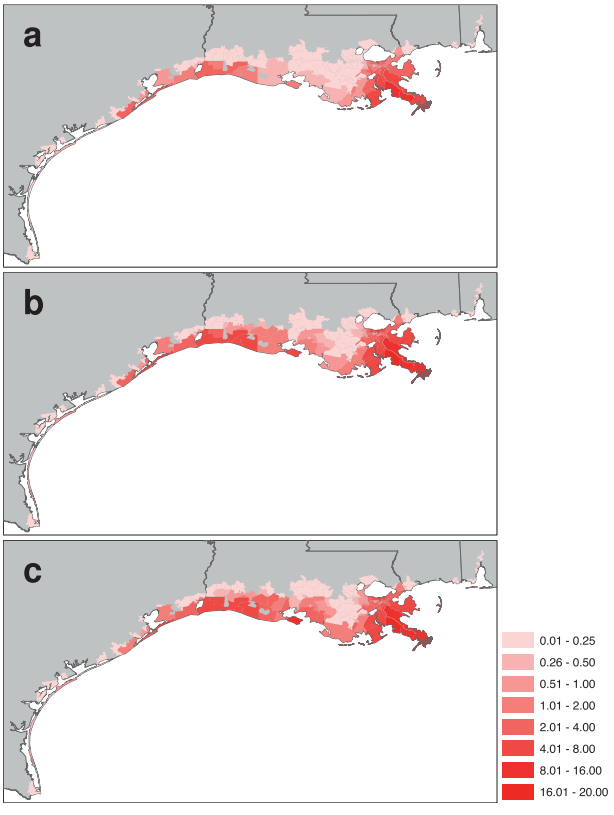


FIG. 15. As in Fig. 10, but for the increase ($/1000) in ground up loss cost relative to the Baseline Scenario along the Gulf Coast for the (a) Full, (b) Full + WSST UB, and (c) Reduced + WSST UB Scenarios.

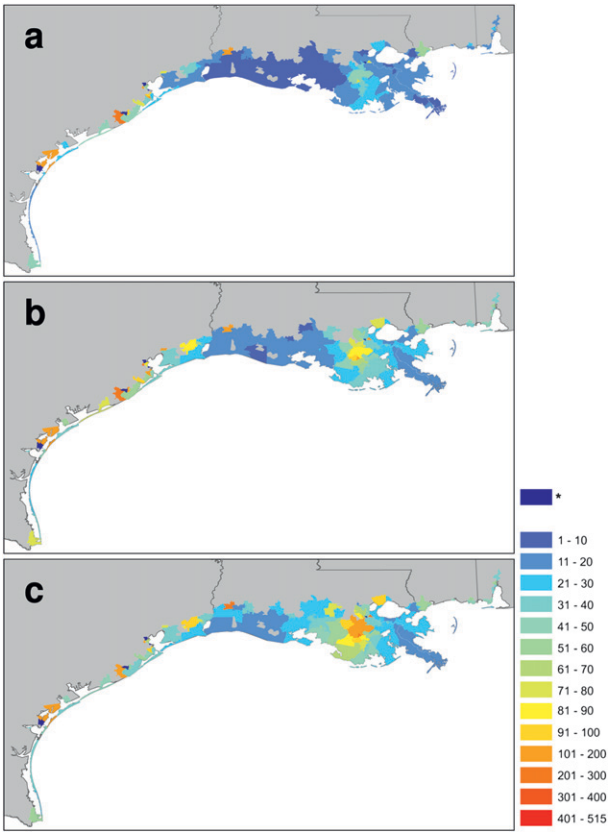


FIG. 16. As in Fig. 11, but for the percentage change in ground up loss cost relative to the Baseline Scenario along the Gulf Coast for the (a) Full, (b) Full + WSST UB, and (c) Reduced + WSST UB Scenarios.

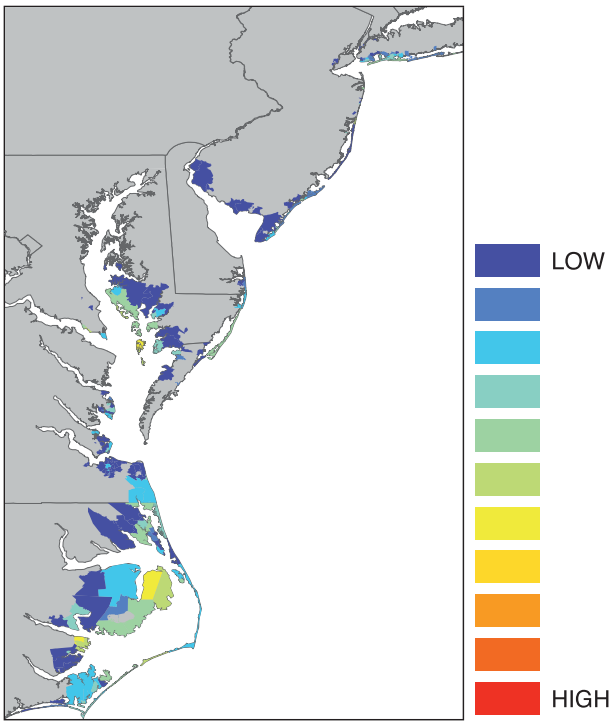


FIG. 17. As in Fig. 9, but for the Baseline Scenario ground up loss cost ($/1000) along the mid-Atlantic coast.

increases. The greatest percentage increases, of roughly 100%, occur for the mid-Atlantic region for the 50-yr return period losses.

- On a local basis, regions most at risk are centered on the Mississippi Delta, the Gulf Coast of Florida south of Tampa Bay, and Cape Hatteras. The regions centered on the Mississippi Delta and Cape Hatteras are also areas where sea level is rising most quickly because of oil and gas extraction, erosion, and sediment loading in the first case, and because of the elastic deformation of the earth's crust associated with the end of the last glaciation in the second case.
- As we found with the regions, zip codes that already have the largest dollar losses also have the largest projected dollar increases, but the smallest projected percentage increases. This pattern does not, however, hold for the mid-Atlantic region where Cape Hatteras localities have both the largest dollar and percentage increases in the WSST cases. This is due to a higher frequency of intense storms making landfall in this region.

The variability in the results of our experiment can be understood in terms of two factors. The first is that losses to property are limited by property values. The generic "damage function" is defined by two intensity levels, the intensity at which damage first occurs and the intensity at which total destruction occurs. In between these two intensity levels, damage follows a logistic growth curve. For individual structural elements, the two intensity levels may be close together, but for an entire structure composed of many elements of varying vulnerability to the hazard, the critical intensity levels spread out. The key here is that at higher intensity levels the logistic growth curve asymptotes at the level of maximum loss (100%) and percentage increases in damage are less than at lower levels of intensity for the same increase in intensity. The

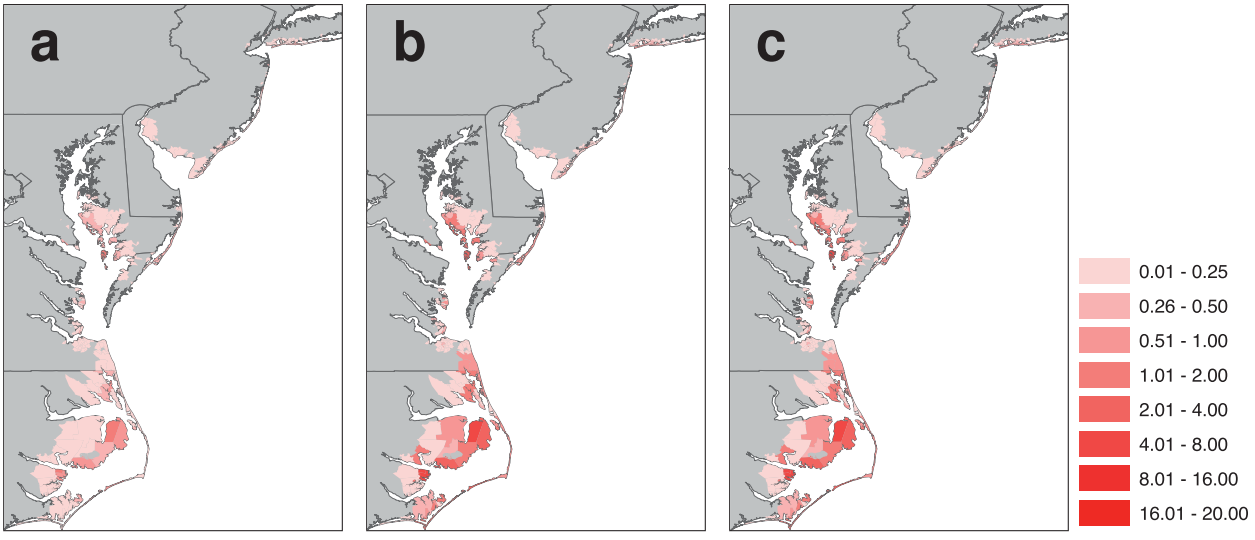


FIG. 18. As in Fig. 10, but for the increase ($/1000) in ground up loss cost relative to the Baseline Scenario along the mid-Atlantic Coast for the (a) Full, (b) Full + WSST UB, and (c) Reduced + WSST UB Scenarios.

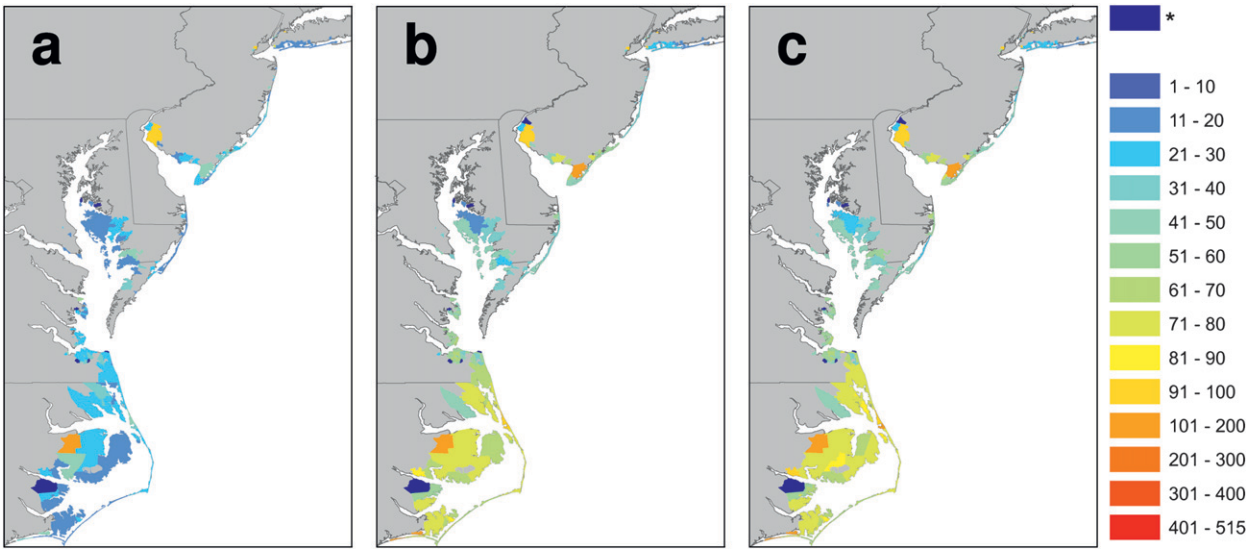


FIG. 19. As in Fig. 11, but for the percentage change in ground up loss cost relative to the Baseline Scenario along the mid-Atlantic Coast for the (a) Full, (b) Full + WSST UB, and (c) Reduced + WSST UB Scenarios.

other factor operating is that the WSST catalog preferentially increases landfall probabilities along the East Coast.

A number of future extensions to the current study are worth pursuing. First, the projection of sea level could be based on climate model simulations. An ensemble of such projections could provide a range of future scenarios, thus accounting for uncertainty in these models. For example, these projections could capture local uncertainties associated with differences among the simulation in ocean circulation, melting of ice caps, and emission scenarios. A number of recent studies have found that changes to ocean circulation, especially to the mean meridional overturning and the subtropical/subpolar gyre circulations (i.e., the upper-ocean basinwide flow that includes the Gulf Stream) (e.g., Hu et al. 2009) and the reduction of the gravitational attraction of the West Antarctic Ice Sheet if it were to melt (e.g., Mitrovica et al. 2009) might have relatively large-amplitude implications for the mid-Atlantic and New England regions. There remains a large uncertainty in parameterizing the physics of ice cap melting, but maximum flow rates for Greenland have been estimated by Pfeffer et al. (2008) that correspond to rates of total sea level rise in the range of 8–20 mm $yr^{-1}$ through the end of the century. These factors would change our estimates of risk as well as increase the uncertainty of our estimates. Second, alternative projections of future hurricane activity could be included. Factors other than SST are known to be important to hurricane activity; the historical record could be stratified by area-averaged maximum potential intensity, depth of the thermocline, or some combination of such parameters. Climate model output could be used here as well. The recent consensus of Knutson et al. (2010) indicates that climate models project fewer tropical disturbances, but more intense tropical cyclones. Climate models can be used to project hurricane statistics or the technique of Emanuel et al. (2008) could be used to develop future hurricane catalogs of sufficient size based on different climate model projections. Third, projections of future property values based on current trends in population shifts, development and zoning regulations, and general economic activity could be included in the analysis. Fourth, changes in construction techniques are likely to make buildings more resilient in the future and this should be factored in as well.

In closing, we observe that when it comes to climate change, simple answers are few and not sufficient to allow for precise projections. But society need not wait until all the answers are known with certainty in order to act. Rather, society must make critical risk management decisions in the face of uncertainty. Evaluating potential actions requires the tools to assess the impact that each action may have. A valuable approach is to inform decision makers with sensitivity studies and potential future scenarios to enable the formation of resilient strategies designed to cope with climate change. The present study is an example of such a tool for stakeholders.

*Acknowledgments.* Tide gauge data used in this study came from the PSMSL and NOAA (NOAA 2007). E. M. Hill and R. M. Ponte were supported by the NASA Grant NNX07AM77G. Additional support at AER was provided by NSF Grant OCE-0961507.


FIG. B1. Domain of the AIR Worldwide Corp. U.S. Hurricane Catastrophe Model.

## APPENDIX A

### Glossary of Insurance Industry Terms

**Average annual loss (AAL)**—Average annual loss, or AAL, refers to the aggregation of losses that can be expected to occur per year, *on average,* over a period of many years. Clearly, significant events will not happen every year; thus, it is important to emphasize that AAL is a *long-term* average.

**Damage Function**—Using mathematical relationships, damage functions describe the relationships between the intensity of an event and damage to the exposed buildings and contents.

**Exposure**—Properties and other insurables that are vulnerable to potential monetary loss from natural hazards or other risk factors.

**Ground up loss**—Total insured losses, including deductibles, before application of any retention or reinsurance. Here, losses to all individual commercial and residential real estate properties do not include losses to so-called in-ground infrastructure, including roadways, utility networks, pipelines, urban transit facilities, and other assets, that might be present in high concentrations in urban areas, and may in fact be insured.

**Industry Exposure Database (IED)**—The Industry Exposure Database contains counts of all insurable properties and their respective replacement values, along with information about occupancy and the physical characteristics of the structures, such as construction type, year built and height classifications. Even information pertaining to standard industry policy conditions, such as limits and deductibles, is incorporated into the database.

**Loss cost**—The expected loss in dollars per thousand of dollars of value in the property inventory.

**Vulnerability**–Susceptibility to sustain damage or loss due to adverse events. Vulnerability is impacted by the construction and occupancy type (e.g., mobile homes are generally more vulnerable than reinforced concrete buildings).

**50-year loss**—The 50-year loss is the loss that has a 2% probability of occurring or being exceeded in any year. Note that the 50-year loss is defined in the context of a given climate regime; that is, the 50-year loss in the current climate regime may be different from the 50-year loss in a future climate regime.

**100-year loss**—The 100-year loss is the loss that has a 1% probability of occurring or being exceeded in any year. Note that the 100-year loss is defined in the context of a given climate regime; that is, the 100-year loss in the current climate regime may be different from the 100-year loss in a future climate regime.

## APPENDIX B

### AIR Hurricane Model for the United States

*a. Description*

The AIR Hurricane Model for the United States captures the effects of hurricane winds and storm surge on

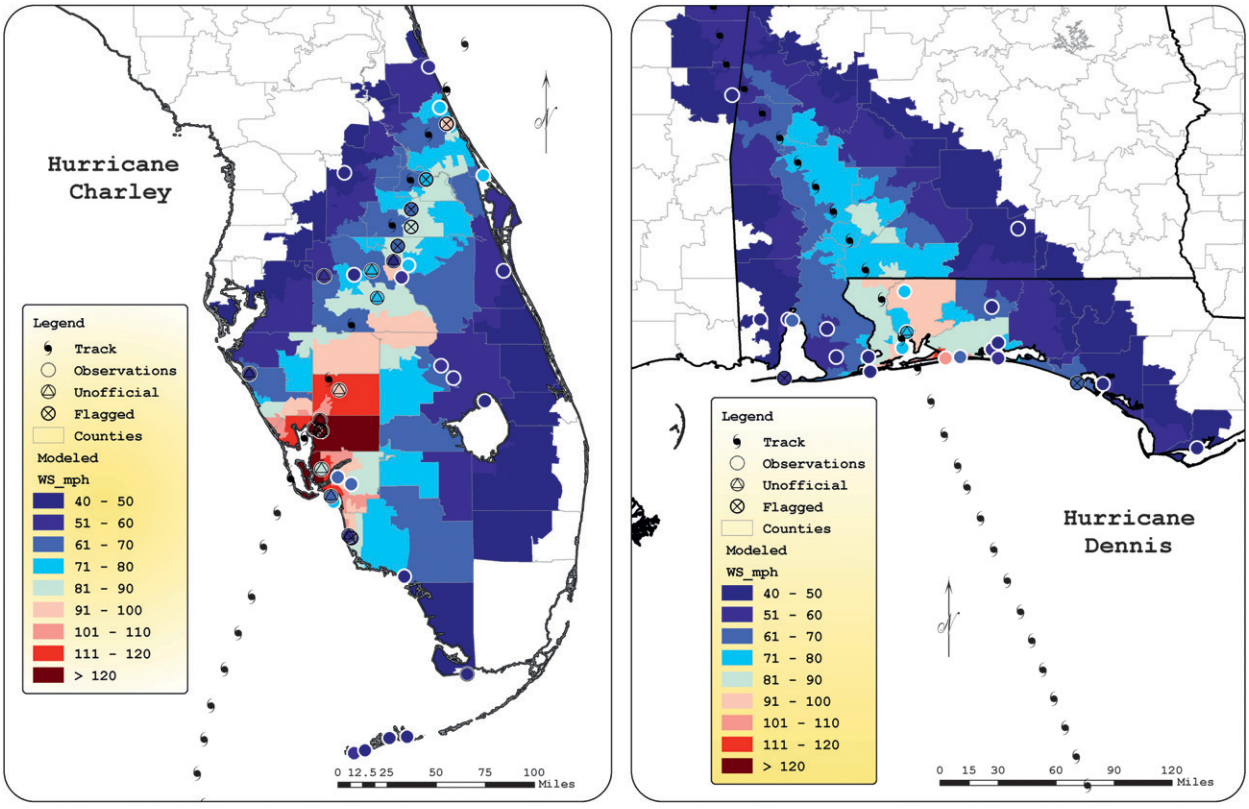


FIG. B2. Observed and modeled wind speeds (mph) for Hurricanes (left) Charley (2004) and (right) Dennis (2005).

insured properties in the United States (for those states plotted with topography in Fig. 6). This is a fully stochastic, event-based model designed for portfolio risk management. Wind intensity computations are based on a storm's intensity, size, location, forward speed, and direction, as well as the underlying terrain and land use in the region. Storm surge is based on the hurricane's meteorological parameters, coastal elevation and geometry, tide heights, and bathymetry. In determining local intensities, the effects of surface friction, filling, and gustiness on wind intensity and attenuation on storm surge are included in order to properly calculate damage to onshore properties. The model is built to meet the wide spectrum of hurricane risk management needs of all stakeholders, including the insurance and reinsurance industry, and accounts for insurance policy conditions specific to the United States.

### b. *Modeled peril*

Wind speeds of ~18 m $s^{-1}$ and above (60-s sustained wind at 10 m) are generally required for potentially damaging conditions that generate losses. The storm surge associated with the wind events is modeled by generating a storm surge profile. The surge profile is modified to account for forward speed, track angle at landfall, bathymetry, astronomical tide, and bay amplification. After the storm surge reaches the coastline, its forward travel is impeded by the friction it experiences from the local terrain. This loss of momentum is referred to as attenuation. Steeper slopes and rougher terrain lead to more rapid attenuation; gradual slopes and smoother terrain lead to slower attenuation. To estimate water depth at each affected location onshore, storm surge is propagated inland using these relationships.

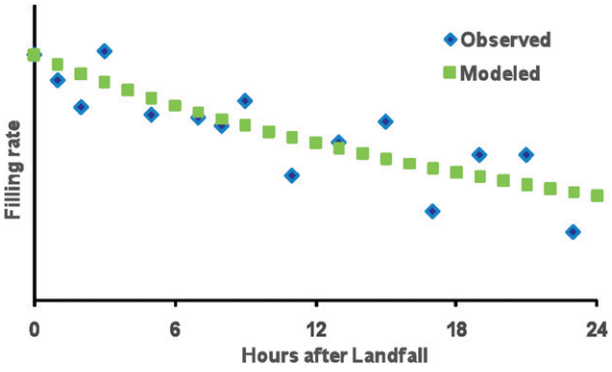


FIG. B3. Actual vs modeled filling rates (hPa $hr^{-1}$) for 2004–05 U.S. landfalling hurricanes.

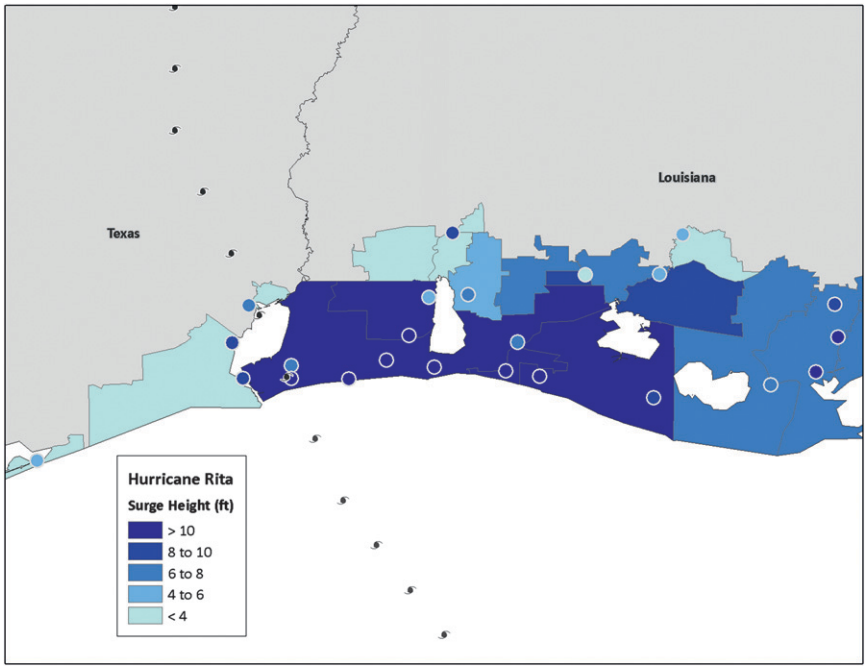


FIG. B4. Comparison between observed (colored circles) and modeled (colored zip codes) storm surge heights for Hurricane Rita (2005). Note that entire zip codes are shaded for the modeled surge heights as computed with respect to the location (and elevation) of the population-weighted zip code centroid.

### c. *Model domain and resolution*

The model domain covers an area from 5°N, 135°W to 65°N, 35°W (Fig. B1). The model resolution is at the U.S. zip code level. Zip codes are polygons of different sizes, and hence provide a variable-resolution grid. This is convenient as zip codes with smaller areas are generally more populated, inherently allowing finer resolution in regions with higher population densities; coastal zip codes tend to have higher population densities than those further inland. For example, zip codes within 16 km of the coast stretching from Texas to Maine have an average area of 58 $km^2$, with the smallest and largest having areas of 1.65 $km^2$ and 1530 $km^2$, respectively. The local intensity parameter used in the storm surge module of the AIR model is water depth in feet. High-resolution elevation data are critical to the calculation. The native horizontal resolution of the U.S. Geological Survey (USGS) elevation data (see Gesch et al. 2002; Gesch 2007) used to model distances within 8 km from the coast is 30 m and is aggregated to 220 m. The vertical resolution is in decimeters.

### d. *Frequency information*

There are 33 422 simulated tropical cyclones in the standard 10 000-yr catalog, which the model shares with the AIR tropical cyclone model for the Caribbean and the AIR U.S. hurricane model for offshore assets. Of these, 18 174 are U.S.-only events, 16 253 of which make landfall in the United States and 1921 of which bypass the mainland. The maximum number of landfalls in a single simulated year is 10. A single storm can make multiple landfalls.

### e. *Model validation*

In addition to the AIR hurricane model's performance with respect to financial loss (cf. Fig. 5), the model has been subjected to repeated internal and external review over a period of more than 20 years. This model has consistently performed very well in this regard. For example, the Florida Commission on Hurricane Loss Projection Methodology (hereafter Florida Commission; see http://www.sbafla.com/methodology/) approves the model used in this study each year. Among the 34 stringent standards set by the Florida Commission are six meteorological standards. To meet these, AIR must demonstrate that the modeled wind field is consistent with the distribution of observed winds for historical storms. The AIR model has consistently met this standard since the Florida Commission was created in 1995.

The AIR hurricane model uses parameterized wind field and storm surge modules. Since the model is proprietary, the parameterizations themselves cannot be

revealed in detail. However, to demonstrate model skill, Fig. B2 shows a comparison between observed and modeled wind speeds for Hurricanes Charley (2004) and Dennis (2005). The simulated wind fields compare very well to observations as do the simulated losses to the claims data (not shown). This level of agreement with observations requires an accurate rate of storm filling (i.e., the rate at which a storm decays or weakens with increasing inland penetration). Figure B3 shows that the modeled filling rates for 2004–05 hurricanes are consistent with those observed. The observations in Fig. B3 consist of intensity information from the Atlantic basin hurricane database (HURDAT), supplemented with landfall data from Blake et al. (2007).

Of critical importance to the current study is the storm surge module of the AIR hurricane model. Some of the parameterizations used here were developed using the NOAA Sea, Lakes, and Overland Surge from Hurricanes (SLOSH) model. As with the wind module, the surge module has been comprehensively evaluated and produces valid results for historical storms. For example, Fig. B4 shows a comparison between observed and modeled storm surge heights for Hurricane Rita (2005). Although the modeled surge heights are represented at the zip code level, the values compare well with observed surge observations. It should be noted again here that, although a single surge height value is likely not valid across an entire zip code, the primary purpose of the hurricane model is to produce accurate loss estimates, which is achieved using this strategy.

(The description in this appendix was adapted from AIR Worldwide Corporation proprietary technical reports describing the AIR Hurricane Model for the U.S. and Offshore Assets.)

## REFERENCES


Bender, M. A., I. Ginis, R. Tuleya, B. Thomas, and T. Marchok, 2007: The operational GFDL coupled hurricane–ocean prediction system and a summary of its performance. *Mon. Wea. Rev.,* **135,** 3965–3989.

——, T. R. Knutson, R. E. Tuleya, J. J. Sirutis, G. A. Vecchi, S. T. Garner, and I. M. Held, 2010: Modeled impact of anthropogenic warming on the frequency of intense Atlantic hurricanes. *Science,* **327,** 454–455, doi:10.1126/science.1180568.

Blake, E. S., E. N. Rappaport, and C. W. Landsea, 2007: The deadliest, costliest, and most intense United States tropical cyclones from 1851 to 2006 (and other frequently requested hurricane facts). NOAA Tech. Memo. NWS TPC-5, 45 pp. [Available online at http://www.aoml.noaa.gov/hrd/Landsea/Blakeetal_noaamemoApr2007.pdf.]

Calais, E., J. Y. Han, C. DeMets, and J. M. Nocquer, 2006: Deformation of the North American plate interior from a decade of continuous GPS measurements. *J. Geophys. Res.,* **111,** B06402, doi:10.1029/2005JB004253.

Cazenave, A., and R. S. Nerem, 2004: Present-day sea level change: Observations and causes. *Rev. Geophys.,* **42,** RG3001, doi:10.1029/2003RG000139.

Church, J. A., and N. J. White, 2006: A 20th century acceleration in global sea-level rise. *Geophys. Res. Lett.,* **33,** L01602, doi:10.1029/2005GL024826.

Dailey, P. S., G. Zuba, G. Ljung, I. M. Dima, and J. Guin, 2009: On the relationship between North Atlantic sea surface temperatures and U.S. hurricane landfall risk. *J. Appl. Meteor. Climatol.,* **48,** 111–129.

Donnelly, J. P., and J. D. Woodruff, 2007: Intense hurricane activity over the past 5,000 years controlled by El Niño and the West African monsoon. *Nature,* **447,** 465–468.

Dunion, J. P., and C. S. Velden, 2004: The impact of the Saharan air layer on Atlantic tropical cyclone activity. *Bull. Amer. Meteor. Soc.,* **85,** 353–365.

Egbert, G. D., and R. D. Ray, 2003: Deviation of long-period tides from equilibrium: Kinematics and geostrophy. *J. Phys. Oceanogr.,* **33,** 822–839.

Emanuel, K., 2005: Increasing destructiveness of tropical cyclones over the past 30 years. *Nature,* **436,** 686–688.

——, R. Sundararajan, and J. Williams, 2008: Hurricanes and global warming: Results from downscaling IPCC AR4 simulations. *Bull. Amer. Meteor. Soc.,* **89,** 347–367.

Gesch, D. B., 2007: The national elevation dataset. *Digital Elevation Model Technologies and Applications: The DEM Users Manual,* 2nd ed., D. Maune, Ed., American Society for Photogrammetry and Remote Sensing, 99–118.

——, M. Oimoen, S. Greenlee, C. Nelson, M. Steuck, and D. Tyler, 2002: The national elevation dataset. *Photogramm. Eng. Remote Sens.,* **68,** 5–11.

Hallegatte, S., N. Patmore, O. Mestre, P. Dumas, C. H. J. Corfee-Morlot, and R. M. Wood, 2008: Assessing climate change impacts, sea level rise and storm surge risk in port cities: A case study on Copenhagen. Environment Working Papers 3, Organisation for Economic Co-operation and Development, 52 pp. [Available online at http://www.oecd-ilibrary.org/environment/assessing-climate-change-impacts-sea-level-rise-and-storm-surge-risk-in-port-cities_236018165623.]

Hill, E. M., R. M. Ponte, and J. L. Davis, 2007: Dynamic and regression modeling of ocean variability in the tide-gauge record at seasonal and longer periods. *J. Geophys. Res.,* **112,** C05007, doi:10.1029/2006JC003745.

Holgate, S. J., and P. L. Woodworth, 2004: Evidence for enhanced coastal sea level rise during the 1990s. *Geophys. Res. Lett.,* **31,** L07305, doi:10.1029/2004GL019626.

Hu, A., G. A. Meehl, W. Han, and J. Yin, 2009: Transient response of the MOC and climate to potential melting of the Greenland Ice Sheet in the 21st century. *Geophys. Res. Lett.,* **36,** L10707, doi:10.1029/2009GL037998.

Hye-Mi, K., P. Webster, and J. Curry, 2009: Impact of shifting patterns of Pacific Ocean warming on North Atlantic tropical cyclones. *Science,* **325,** 77–80, doi:10.1126/science.1174062.

Irish, J. L., D. T. Resio, and J. J. Ratcliff, 2008: The influence of storm size on hurricane surge. *J. Phys. Oceanogr.,* **38,** 2003–2013.

Jelesnianski, C. P., 1972: SPLASH (Special Program to List Amplitudes of Surges from Hurricanes): I. Landfall storms. NOAA Tech. Memo. NWS TDL-46, 52 pp.

Kennedy, A. B., S. Rogers, A. Sallenger, U. Gravois, B. C. Zachry, and F. Z. M. Dosa, 2010: Building destruction from waves and surge on the Bolivar Peninsula during Hurricane Ike. *J. Waterw. Port Coastal Ocean Eng.,* doi:10.1061/(ASCE)WW.1943-5460.0000061, in press.

Knutson, T. R., and Coauthors, 2010: Tropical cyclones and climate change. *Nat. Geosci.,* **3,** 157–163, doi:10.1038/ngeo779.

Kug, J.-S., F.-F. Jin, and S.-I. An, 2009: Two types of El Niño events: Cold tongue El Niño and warm pool El Niño. *J. Climate,* **22,** 1499–1515.

Landsea, C. W., 2005: Hurricanes and global warming. *Nature,* **438,** E11–E12, doi:10.1038/nature04477.

Lee, K., and D. V. Rosowsky, 2005: Fragility assessment for roof sheathing failure in high wind regions. *Eng. Structures,* **6,** 857–868.

Leuliette, E. W., R. S. Nerem, and G. T. Mitchum, 2004: Calibration of TOPEX/Poseidon and Jason altimeter data to construct a continuous record of mean sea level change. *Mar. Geod.,* **27,** 79–94.

Mann, M. E., and K. A. Emanuel, 2006: Atlantic hurricane trends linked to climate change. *Eos, Trans. Amer. Geophys. Union,* **87,** doi:10.1029/2006EO240001.

——, ——, G. J. Holland, and P. J. Webster, 2007: Atlantic tropical cyclones revisited. *Eos, Trans. Amer. Geophys. Union,* **88,** doi:10.1029/2007EO360002.

McInnes, K. L., K. J. E. Walsh, G. D. Hubbert, and T. Beer, 2003: Impact of sea-level rise and storm surges on a coastal community. *Nat. Hazards,* **30,** 187–207.

Mitrovica, J. X., N. Gomez, and P. U. Clark, 2009: The sea-level fingerprint of West Antarctic collapse. *Science,* **323,** 753, doi:10.1126/science.1166510.

Morton, R. A., J. C. Bernier, J. A. Barras, and N. F. Ferina, 2005: Rapid subsidence and historical wetland loss in the Mississippi Delta plain: Likely causes and future implications. Rep. 1216, U.S. Geological Survey, 116 pp. [Available online at http://pubs.usgs.gov/of/2005/1216/.]

NOAA, cited 2007: Linear mean sea level (MSL) trends and 95% confidence intervals in mm/yr. NOAA Center for Operational Oceanographic Products and Services. [Available online at http://tidesandcurrents.noaa.gov/sltrends/msltrendstable.htm.]

Pachauri, R. K., and A. Reisinger, Eds., 2007: *Climate Change 2007: Synthesis Report*. Intergovernmental Panel on Climate Change, 104 pp. [Available online at http://www.ipcc.ch/publications_and_data/publications_ipcc_fourth_assessment_report_synthesis_report.htm.]

Pfeffer, W. T., J. T. Harper, and S. O'Neel, 2008: Kinematic constraints on glacier contributions to 21st-century sea-level rise. *Science,* **321,** 1340–1343, doi:10.1126/science.1159099.

Ponte, R. M., 2006: Low frequency sea level variability and the inverted barometer effect. *J. Atmos. Oceanic Technol.,* **23,** 619–629.

Rosowsky, D. V., and B. R. Ellingwood, 2002: Performance-based engineering of wood frame housing: A fragility analysis methodology. *J. Struct. Eng.,* **128,** 32–38.

Sabbatelli, T. A., and M. E. Mann, 2007: The influence of climate state variables on Atlantic tropical cyclone occurrence rates. *J. Geophys. Res.,* **112,** D17114, doi:10.1029/2007JD008385.

Saunders, M. A., R. E. Chandler, C. J. Merchant, and F. P. Roberts, 2000: Atlantic hurricanes and NW Pacific typhoons: ENSO spatial impacts on occurrence and landfall. *Geophys. Res. Lett.,* **27,** 1147–1150.

Shepherd, J. M., and T. Knutson, 2007: The current debate on the linkage between global warming and hurricanes. *Geogr. Compass,* **1,** 1–24, doi:10.1111/j.1749-8198.2006.00002.x.

Sill, B. L., and R. T. Kozlowski, 1997: Analysis of storm damage factors for low rise structures. *J. Perform. Constr. Facil.,* **11,** 168–177.

Solomon, S., D. Qin, M. Manning, M. Marquis, K. Averyt, M. M. B. Tignor, H. L. Miller Jr., and Z. Chen, Eds., 2007: *Climate Change 2007: The Physical Science Basis*. Cambridge University Press, 996 pp.

Swanson, K. L., 2008: Nonlocality of Atlantic tropical cyclone intensities. *Geochem. Geophys. Geosyst.,* **9,** Q04V01, doi:10.1029/2007GC001844.

Unanwa, C. O., J. R. McDonald, K. C. Mehta, and D. A. Smith, 2000: The development of wind damage bands for building. *J. Wind Eng. Ind. Aerodyn.,* **84,** 119–149.

Vecchi, G. A., and T. R. Knutson, 2008: On estimates of historical North Atlantic tropical cyclone activity. *J. Climate,* **21,** 3580–3600.

Woodworth, P. L., and D. L. Blackman, 2004: Evidence for systematic changes in extreme high waters since the mid-1970s. *J. Climate,* **17,** 1190–1197.

Zervas, C., 2001: Sea level variations of the United States 1854–1999. NOAA Tech. Rep. NOS CO-OPS 36, 80 pp + appendices. [Report available online at http://tidesandcurrents.noaa.gov/publications/techrpt36doc.pdf; appendices available at http://tidesandcurrents.noaa.gov/pub.html.]

Zhang, K., B. C. Douglas, and S. P. Leatherman, 2000: Twentieth-century storm activity along the U.S. East Coast. *J. Climate,* **13,** 1748–1761.